ELSEVIER

Probabilistic Engineering Mechanics 21 (2006) 112–132

PROBABILISTIC ENGINEERING MECHANICS

www.elsevier.com/locate/probengmech

Material spatial randomness: From statistical to representative volume element☆

Martin Ostoja-Starzewski *

Department of Mechanical Engineering, and McGill Institute for Advanced Materials, McGill University, Montreal, Que. H3A 2K6, Canada

Received 4 November 2004; received in revised form 30 June 2005; accepted 27 July 2005
Available online 20 October 2005

Abstract

The material spatial randomness forces one to re-examine various basic concepts of continuum solid mechanics. In this paper we focus on the Representative Volume Element (RVE) that is commonly taken for granted in most of deterministic as well as in stochastic solid mechanics, although in the latter case it is called the Statistical Volume Element (SVE). The key issue is the scale over which homogenization is being carried out—it is called the mesoscale, separating the microscale (level of microheterogeneities) from the macroscale (level of RVE). As the mesoscale grows, the SVE tends to become the RVE. This occurs in terms of two hierarchies of bounds stemming from Dirichlet and Neumann boundary value problems on the mesoscale, respectively. Since generally there is no periodicity in real random media, the RVE can only be approached approximately on finite scales. We review results on this subject in the settings of linear elasticity, finite elasticity, plasticity, viscoelasticity, thermoelasticity, and permeability.

Keywords: Random media; Representative volume element; Statistical volume element; Scale effects

1. Introduction

1.1. Separation of scales

Continuum mechanics hinges on the concept of a *Representative Volume Element* (RVE) playing the role of a mathematical point of a continuum field approximating the true material microstructure. The RVE is very clearly defined in two situations only: (i) unit cell in a periodic microstructure, and (ii) volume containing a very large (mathematically infinite) set of microscale elements (e.g. grains), possessing statistically homogeneous and ergodic properties. The approach via unit cell is, strictly speaking, restricted to materials displaying periodic geometries. When we consider case (ii) we intuitively think of a medium with microstructure so fine we cannot see it—naturally then we envisage a *homogeneous deterministic continuum* in its place. This situation, as suggested by Fig. 1, is called a *separation of scales*

$$\left.\begin{matrix} d< \\ d\ll \end{matrix}\right\} L \ll L_{\text{macro}}, \tag{1.1}$$

and introduces three scales:

- the *microscale d*, such as the average size of grain (or inclusion, crystal, etc.) in a given microstructure; we initially assume the microstructures to be characterized by just one size d;
- the *mesoscale L*, size of the RVE (if so justified—see below);
- the *macroscale* L_{macro}, macroscopic body size.

In (1.1) on the left we do admit two options, because the inequality $d<L$ may be sufficient for microstructures with weak geometric disorder and weak mismatch in properties; otherwise a much stronger statement $d\ll L$ applies. Note also that the first inequality in $(1.1)_1$ could even be a weak one because we may be considering a microstructure with a nearly periodic geometry, though possessing some randomness on the level of the unit cell.

In any case, the issue of central concern is the trend—either rapid, moderate, or slow—of mesoscale constitutive response, with L/d increasing, to the situation postulated by Hill [1]: "a sample that (a) is structurally entirely typical of the whole mixture on average, and (b) contains a sufficient number of inclusions for the apparent overall moduli to be effectively

☆ Keynote lecture at International Conference on Heterogeneous Material Mechanics, China, 2004.

* Corresponding author. Tel.: +1 514 398 7394; fax: 1 514 398 7365.
E-mail address: martin.ostoja@mcgill.ca.

0266-8920/$ - see front matter © 2005 Elsevier Ltd. All rights reserved.
doi:10.1016/j.probengmech.2005.07.007

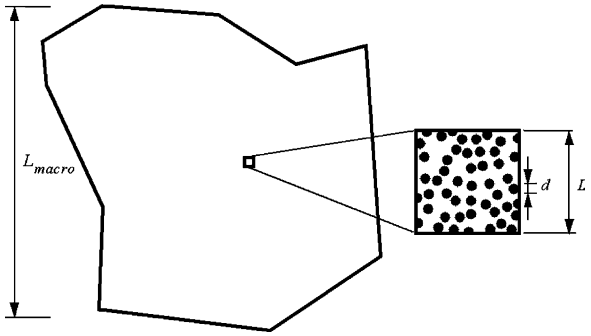

Fig. 1. A macroscopic body of size L_{macro} with a mesoscale window of size L, in which a microstructure of size d is shown. δ-Dependence of apparent moduli of a disk-matrix composite at contrasts $C^{(i)}/C^{(m)}=10$ (a) and $C^{(i)}/C^{(m)}=1000$ (b), at volume fraction 35%, under boundary conditions (2.11)–(2.16).

independent of the surface values of traction and displacement, so long as these values are macroscopically uniform." In essence, (a) is a statement about the material's statistics, while (b) is a pronouncement on the independence of effective constitutive response with respect to the boundary conditions. Both of these are issues of mesoscale L of the domain of random microstructure over which smoothing (or homogenization) is being done relative to the microscale d and macroscale L_{macro}. These considerations, however, are not rigorous, because neither spatial statistics nor mechanics (or physics) definitions of properties have yet been introduced.

1.2. Basic concepts

A note on determinism. In principle, any realization $B(\omega)$ of the composite $\mathcal{B}=\{B(\omega);\omega\in\Omega\}$, while spatially disordered (i.e. heterogeneous), follows deterministic laws of mechanics. The most preferred approach, dictated by stochastic mechanics, would be to first ascertain what happens to each and every $B(\omega)$ of $\mathcal{B}$, starting from a certain random microstructure model, and then pass to ensemble setting, by taking the averages or higher moments as the need arises. In most situations, however, this may generate enormous amounts of perhaps not very useful information.

Ensemble versus volume averaging. We reserve the overbar for spatial (volume or areal) averages, and $\langle\cdot\rangle$ for ensemble averages. That is, if we have a random (n-component, real valued) field Θ defined over some probability space $\{\Omega, F, P\}-F$ being a σ-field and P a probability measure—over some domain X in $\mathbb{R}^D$ of volume V

$$\Theta:\Omega\times X\to\mathbb{R}^n, \tag{1.2}$$

the said averages are

$$\overline{\Theta(\omega)}\equiv\frac{1}{V}\int_V\Theta(\omega,\mathbf{x})\mathrm{d}V\qquad\langle\Theta(\mathbf{x})\rangle\equiv\int_\Omega\Theta(\omega,\mathbf{x})\mathrm{d}P. \tag{1.3}$$

We assume the conditions necessary for the fulfillment of commutativity of both operations to be satisfied (i.e. requirements of Fubini's theorem) so that

$$\langle\overline{\boldsymbol{\Theta}}\rangle=\overline{\langle\boldsymbol{\Theta}\rangle}. \tag{1.4}$$

Tensor notation. Clearly, upon taking the spatial average, the dependence on position $\mathbf{x}$ vanishes, while upon taking the ensemble average, the dependence on ω vanishes. A tensor of, say, second order is denoted symbolically by $\mathbf{t}$ and, in index notation, by t_{ij}. Both notations are used interchangeably, as are the scalar product operations

$$\mathbf{t}\cdot\mathbf{n},\quad\mathbf{t}:\mathbf{a},\quad\mathbf{C}:\mathbf{a}, \tag{1.5}$$

and, respectively,

$$t_{ij}n_j,\quad t_{ij}a_{ij},\quad C_{ijkl}a_{kl}, \tag{1.6}$$

when the need arises.

1.3. The RVE postulate

The random material on *mesoscale*, such as shown in Fig. 1, is denoted $\mathcal{B}_{L/d}=\{B_{L/d}(\omega);\omega\in\Omega\}$ with $B_{L/d}(\omega)$ being one realization. Properties on mesoscale are also described by an adjective *apparent* [2], as opposed to *effective*. The latter term pertains to the limit $L/d\to\infty$ as it connotes the passage to the RVE, while any finite mesoscale involves statistical scatter and, therefore, describes some *Statistical Volume Element* (SVE). Note here that the RVE postulate as well as the separation of scales are also known in the solid mechanics literature as the *MMM principle* [3].

In the following, it will be convenient to describe the mesoscale by a nondimensional parameter

$$\delta=L/d \tag{1.7}$$

in the range $[1,\infty]$, so that $\mathcal{B}_{L/d}$ will be written $\mathcal{B}_\delta$, etc.

The setting is one of quasi-static loading, so that the body is governed locally by the equilibrium equation

$$\sigma_{ij,j}=0, \tag{1.8}$$

where σ_{ij} is the Cauchy stress, body forces being disregarded.

For a mesoscale body $B_\delta(\omega)$ of volume V_δ, such as the microstructure shown in Fig. 1, we define volume average stress and strain

$$\bar{\sigma}_\delta(\omega)=\frac{1}{V_\delta}\int\sigma(\omega,\mathbf{x})\mathrm{d}V\quad\bar{\varepsilon}_\delta(\omega)=\frac{1}{V_\delta}\int\varepsilon(\omega,\mathbf{x})\mathrm{d}V. \tag{1.9}$$

Assuming we deal with a linear elastic microstructure, the problem is to pass from the random field of stiffness with fluctuations on the microscale

$$\sigma=\mathbf{C}(\omega,\mathbf{x}):\varepsilon,\quad\omega\in\Omega,\quad\mathbf{x}\in B \tag{1.10}$$

to some effective Hooke's law

$$\bar{\sigma}_\delta=\mathbf{C}^{\mathrm{eff}}:\bar{\varepsilon}_\delta, \tag{1.11}$$

whereby (a) the dependence on ω (i.e. randomness) would be removed, (b) the dependence on $\mathbf{x}$ (i.e. spatial fluctuations) of strain and stress fields would also vanish, and (c) the independence of response with respect to boundary conditions would be attained. It is intuitively expected that δ needs to be large, but exactly how large it should be, is the key question.

Suppose we are tackling a boundary value problem of a body on macroscopic length scales. In general situations we have to use computational mechanics—such as, say, a finite element meshing of the body—and this approach conventionally assumes that every single finite element is at least as large as the RVE, although this is rarely verified. Thus, there arises a need to know the rate of approach of SVE to RVE in function of δ, phases' mismatch, phases' microgeometry, etc. and, whether that rate is too slow in a given problem. If the latter is the case, one then needs to set up a stochastic finite element (SFE) scheme to account for the microstructural noise on the mesoscale of any given finite element, e.g. [4]. In this paper we will not discuss such SFE, but only focus on the passage from SVE to RVE. Let us note here that the typical recipes of solid mechanics (e.g. [5]) vaguely say that δ of RVE should be about 10–100, but the analyses reported below show that it strongly depends on the type of problem studied.

A review of results on the subject of scaling from SVE up to RVE in the setting of single-scale (not multi-scale) heterogeneous media, defines the goal of this paper; it updates the results collected in [6]. The review is not complete, principally because other definitions of the RVE than that employed here—without the concept of SVE—have been introduced in the literature, e.g. [7,8,72,73].

Let us end this section with an observation that in problems of high strain/stress gradients, the length scale defined by the deformation field may easily become of the order of d (i.e. $\delta \to 1$), and the homogenization to RVE in the sense proposed here would then not be recommended, as too much detail would be lost. Second-order hamogenization is then needed [74–76].

2. Volume averaging

2.1. A paradigm of boundary conditions effect

Clearly, the attainment of the RVE is a function of the scale δ as well as the mismatch in properties of inclusions versus matrix. To illustrate this point, let us consider boundary distributions of displacement u_3 and stress traction t_3 in two boundary value problems of the mesoscale window $B_\delta(\omega)$ of matrix-inclusion specimen of Fig. 1 (now shown in Fig. 2) in anti-plane elasticity. The material is piecewise uniform with perfectly bonded, isotropic phases, so that the governing equation is

$$C^{(p)}\nabla^2 u = 0 \qquad p = m, i. \tag{2.1}$$

Here m and i denote matrix and inclusion respectively, and $C_{3i3j} = C^{(p)}\delta_{ij}$ (δ_{ij} is the Kronecker delta) is the phase stiffness. Two boundary value problems are considered: one of Dirichlet type

$$u_3(\mathbf{x}) = \varepsilon^0_{3i}x_i \qquad \forall\, \mathbf{x} \in \partial B_\delta, \tag{2.2}$$

where the strain ε^0_{3j} is prescribed, and the other of Neumann type

$$t_3(\mathbf{x}) = \sigma^0_{3j}n_j \qquad \forall\, \mathbf{x} \in \partial B_\delta, \tag{2.3}$$

where the stress σ^0_{3j} is prescribed. Here (B_δ denotes the boundary of B_δ.

Fig. 2(a) treats the situation of no mismatch in the material properties: $C^{(i)}/C^{(m)} = 1$. and so we we can interpret it as either a uniform displacement field on the boundary (B_δ under $\varepsilon^0 = (\varepsilon^0_{31}, \varepsilon^0_{32})c$, with $\varepsilon^0_{32} = 0$, resulting in a uniform stress field on (B_δ, or a uniform stress field on (B_δ under $\sigma^0 = (\sigma^0_{31}, \sigma^0_{32})$, with $\sigma^0_{32} = 0$, resulting in a uniform displacement field on (B_δ. Evidently, both problems are perfectly interchangeable because the microstructure is trivially homogeneous. This then is the trivial situation of the RVE.

Both boundary value problems become much more interesting when $C^{(i)}/C^{(m)} \neq 1$. In Fig. 2 (b–d) we decrease

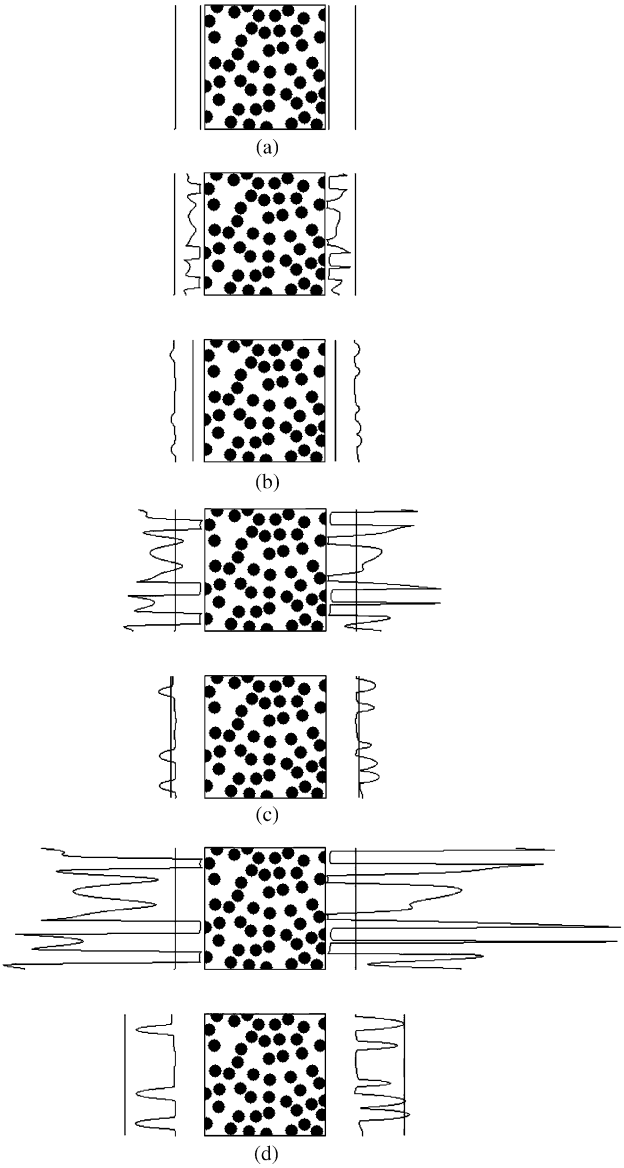

Fig. 2. Anti-plane elastic responses of a matrix-inclusion composite, with nominal 35% volume fraction of inclusions, at decreasing contrasts: (a) $C^{(i)}/C^{(m)} = 1$, (b) $C^{(i)}/C^{(m)} = 0.2$, (c) $C^{(i)}/C^{(m)} = 0.05$, (d) $C^{(i)}/C^{(m)} = 0.02$. For (b–d), the first figure shows response under Dirichlet boundary conditions, while the second shows response under Neumann boundary conditions with $\boldsymbol{\sigma}^0$ equal to the volume average $\bar{\sigma}$ of stress computed in the Dirichlet problem.

the mismatch by first setting it to 0.2, then 0.05, and finally 0.02. In each case, we first solve the Dirichlet problem under $\varepsilon^0 = (\varepsilon^0_{31}, 0)$, and find $\mathbf{t}(\mathbf{x})$. Next, we compute the volume average $\mathbf{t}^-$ of $\mathbf{t}(\mathbf{x})$ on (B_δ, and set $\mathbf{t}^0 = \bar{\mathbf{t}}$ to run the Neumann problem. We keep ε^0 identical in all four cases (a–d).

Let us now define an 'apparent stiffness' $\mathbf{C}^d$ in the displacement controlled (^{d}) problem (2.2) via equation

$$\bar{\sigma} = \mathbf{C}^d : \varepsilon^0, \tag{2.4}$$

and 'apparent compliance' $\mathbf{S}^t$ in the Neumann (^{t}) problem (2.3) via equation

$$\bar{\varepsilon} = \mathbf{S}^t : \sigma^0. \tag{2.5}$$

The latter allows us to define 'apparent stiffness' in the traction controlled problem as $\mathbf{C}^t = (\mathbf{S}^t)^{-1}$.

The following points are noteworthy:

(i) the volume average displacement of the resulting $u_3(\mathbf{x})$ distribution in the problem (2.2) differs from that in the problem (2.3);
(ii) the 'apparent stiffness' in one boundary value problem is different from that in the other one; this should not be surprising given the preceding observation;
(iii) the degree to which $\mathbf{C}^d$ is different from $(\mathbf{S}^t)^{-1}$ may be regarded as an indication of the departure from the effective moduli $\mathbf{C}^{\text{eff}}$ in separation of scales; as a measure of their closeness to $\mathbf{C}^{\text{eff}}$ one might use the deviation of the product $\mathbf{C}^d$: $\mathbf{S}^t$ from unity;
(iv) while the governing partial differential equation is linear (and we could even replace (2.1) by $(C_{ij}u_{3,j})_{,i} = 0$), the resulting property is nonlinear as a function of actual realization ω, scale δ, mismatch $C^{(i)}/C^{(m)}$, and type of boundary conditions (i.e. Dirichlet or Neumann) [9].

2.2. Hill Condition

2.2.1. Mechanical versus energy definitions

Let us consider a body $B_\delta(\omega)$ with a given microstructure, in which, as a result of some boundary conditions and in the absence of body forces, there are stress and strain fields $\boldsymbol{\sigma}$ and ε. If we represent them as a superposition of the means ($\bar{\sigma}$ and $\bar{\varepsilon}$) with zero-mean fluctuations ($\boldsymbol{\sigma}'$ and $\boldsymbol{\varepsilon}'$)

$$\sigma(\omega, \mathbf{x}) = \bar{\sigma} + \sigma'(\omega, \mathbf{x}) \qquad \varepsilon(\omega, \mathbf{x}) = \bar{\varepsilon} + \varepsilon'(\omega, \mathbf{x}), \tag{2.6}$$

we find for the volume average of the energy density over $B_\delta(\omega)$

$$\bar{U} \equiv \frac{1}{2V} \int_{B_\delta(\omega)} \sigma(\omega, \mathbf{x}) : \varepsilon(\omega, \mathbf{x}) dV = \frac{1}{2}\overline{\sigma : \varepsilon} = \frac{1}{2}\bar{\sigma} : \bar{\varepsilon} + \frac{1}{2}\overline{\sigma' : \varepsilon'}. \tag{2.7}$$

Thus, we see that for the average of a scalar product of stress and strain fields to equal the product of their averages

$$\overline{\sigma : \varepsilon} = \bar{\sigma} : \bar{\varepsilon}, \tag{2.8}$$

we need

$$\overline{\sigma' : \varepsilon'} = 0. \tag{2.9}$$

Relation (2.8) is called the *Hill condition* in the (conventional) volume average form ([1]; see also [10–15]). Some authors (e.g. [16]) call it the *Hill-Mandel macrohomogeneity condition*, after J. Mandel.

For an unbounded space domain ($\delta \to \infty$), (2.8) is trivially satisfied, but for a finite body it requires that the body be loaded in a specific way on its boundary (B_δ. Following Hazanov & Amieur [17], by the Green-Gauss theorem, we find the necessary and sufficient condition for (2.8) to hold

$$\overline{\sigma : \varepsilon} = \bar{\sigma} : \bar{\varepsilon} \Leftrightarrow \int_{\partial B_\delta} (\mathbf{t} - \bar{\sigma}\cdot\mathbf{n})\cdot(\mathbf{u} - \bar{\varepsilon}\cdot\mathbf{x}) \mathrm{d}S = 0. \tag{2.10}$$

This is satisfied by three different types of boundary conditions on the mesoscale: *uniform displacement* (also called kinematic, essential, or Dirichlet) boundary condition (*dd*)

$$\mathbf{u}(\mathbf{x}) = \varepsilon^0 \cdot \mathbf{x} \qquad \forall\, \mathbf{x} \in \partial B_\delta; \tag{2.11}$$

uniform traction (also called static, natural, or Neumann) boundary condition (*tt*)

$$\mathbf{t}(\mathbf{x}) = \sigma^0 \cdot \mathbf{n} \qquad \forall\, \mathbf{x} \in \partial B_\delta; \tag{2.12}$$

uniform displacement-traction (also called orthogonal-mixed) boundary condition (dt)

$$(\mathbf{t}(\mathbf{x}) - \sigma^0\cdot\mathbf{n})\cdot(\mathbf{u}(\mathbf{x}) - \varepsilon^0\cdot\mathbf{x}) = 0 \qquad \forall\, \mathbf{x} \in \partial B_\delta. \tag{2.13}$$

Here we employ $\boldsymbol{\varepsilon}^0$ and $\boldsymbol{\sigma}^0$ to denote constant tensors, prescribed a priori, and note, from the strain average and stress average theorems: $\varepsilon^0 = \bar{\varepsilon}$ and $\sigma^0 = \bar{\sigma}$.

It is highly popular in mechanics of random media to assume some finite scale periodicity of the microstructure, while still keeping spatial disorder. In that case, one can specify *periodic boundary conditions* (*pp*)

$$\mathbf{u}(\mathbf{x} + \mathbf{L}) = \mathbf{u}(\mathbf{x}) + \varepsilon^0 \cdot \mathbf{x} \qquad \mathbf{t}(\mathbf{x} + \mathbf{L}) = -\mathbf{t}(\mathbf{x}) \qquad \forall \mathbf{x} \in \partial B_\delta, \tag{2.14}$$

where $\mathbf{L} = L\mathbf{n}$.

Two other possibilities of mixed boundary conditions [18] include combinations of (2.11), (2.12) and (2.14), namely *displacement-periodic* boundary condition (*dp*)

$$\begin{aligned} &\mathbf{u}(\mathbf{x}) = \varepsilon^0 \mathbf{x} && \forall \mathbf{x} \in \partial B^d_\delta \\ &\mathbf{u}(\mathbf{x} + \mathbf{L}) = \mathbf{u}(\mathbf{x}) + \varepsilon^0 \mathbf{x} && \mathbf{t}(\mathbf{x} + \mathbf{L}) = -\mathbf{t}(\mathbf{x}) \quad \forall\, \mathbf{x} \in \partial B^p_\delta \end{aligned} \tag{2.15}$$

traction-periodic boundary condition (*tp*)

$$\begin{aligned} &\mathbf{t}(\mathbf{x}) = \sigma^0 \mathbf{n} && \forall \mathbf{x} \in \partial B^t_\delta \\ &\mathbf{u}(\mathbf{x} + \mathbf{L}) = \mathbf{u}(\mathbf{x}) + \varepsilon^0 \mathbf{x} && \mathbf{t}(\mathbf{x} + \mathbf{L}) = -\mathbf{t}(\mathbf{x}) \quad \forall\, \mathbf{x} \in \partial B^p_\delta \end{aligned} \tag{2.16}$$

Each of these boundary conditions results in a different *mesoscale* (or *apparent*, after Huet) stiffness, or compliance

tensor. Either of these terms is used to make a distinction from the *macroscale* (or *effective, global, overall,…*) properties that are typically denoted by ^{eff} or *, see, e.g. [19].

For a given realization $B_\delta(\omega)$ of the random medium $\mathcal{B}_\delta$, taken as a linear elastic body ($\boldsymbol{\sigma}=\mathbf{C}(\omega,\ \mathbf{x})$: $\boldsymbol{\varepsilon}$), on some mesoscale δ, dispalcement boundary condition (2.11) yields an apparent random stiffness tensor $\mathbf{C}^d_\delta(\omega)$—sometimes denoted $\mathbf{C}^e_\delta(\omega)$—with the constitutive law

$$\bar{\sigma} = \mathbf{C}^d_\delta(\omega) : \varepsilon^0. \tag{2.17}$$

On the other hand, the traction boundary condition (2.12) results in an apparent random compliance tensor $\mathbf{S}^t_\delta(\omega)$—sometimes denoted $\mathbf{S}^n_\delta(\omega)$—with the constitutive law being stated as

$$\bar{\varepsilon} = \mathbf{S}^t_\delta(\omega) : \sigma^0. \tag{2.18}$$

The third type of boundary condition, (2.13), evidently involves a combination of (2.11) and (2.12); it results in a stiffness tensor $\mathbf{C}^{dt}_\delta(\omega)$. In fact, this condition may best represent actual experimental setups. For example, it may signify displacement boundary conditions on two parallel sides, and traction-free boundary conditions on the remaining two parallel sides. Or, it may signify pure shear loading through boundary conditions (see Fig. 3)

$$\varepsilon^0_{11} = -\varepsilon^0_{22} \quad \sigma^0_{12} = 0. \tag{2.19}$$

2.2.2. Order relations dictated by three types of loading

Note from the discussion above that the use of (2.8) assures the equivalence of the properties from the mechanical standpoint—i.e. via apparent Hooke's law (2.11) or (2.12)—with the properties from the energy standpoint.

Both approaches are equivalent for a homogeneous material—i.e. the RVE—but not necessarily so for a heterogeneous one, $B_\delta(\omega)$, of size finite relative to the microscale heterogeneity ($\delta<\omega$). In fact, a following relation ordering the Neumann and Dirichlet apparent moduli holds: $[\mathbf{S}^t_\delta(\omega)]^{-1} \le \mathbf{C}^d_\delta(\omega)$. A proof of the above in the framework of functional analysis has been given in [20], and another one in the framework of general convex analysis applied to nonlinear case [21], which was followed by Huet [13]. Later on, Hazanov and Huet [22] extended it to the following

$$[\mathbf{S}^t_\delta(\omega)]^{-1} \le \mathbf{C}^{dt}_\delta(\omega) \le \mathbf{C}^d_\delta(\omega), \tag{2.20}$$

that is, the modulus of $B_\delta(\omega)$ obtained under the mixed *dt*-conditions (2.13) always lies between the moduli obtained under the *tt*-conditions (2.12) and the *dd*-conditions (2.11). Other consequences of (2.20)—especially, in the context of orthotropic materials—were discussed by [17].

Another important result, also due to [13], is that

$$\langle \mathbf{S}^t_\delta(\omega)\rangle^{-1} \le \mathbf{C}^{\text{eff}}(\omega) \le \langle \mathbf{C}^d_\delta(\omega)\rangle. \tag{2.21}$$

That is, the effective modulus $\mathbf{C}^{\text{eff}}(\omega)$ always lies between the harmonic average of moduli obtained under the Neumann boundary conditions on the ensemble $\mathcal{B}_\delta$ and the arithmetic average of moduli obtained under the Dirichlet conditions on the same ensemble.

Various quantitative estimates of δ-dependence—or, what is called *finite-size scaling* in condensed matter physics—were computed for many different materials by Huet and co-workers, this author and co-workers; see also [26], and [27]. This paper reviews more recent results on this subject.

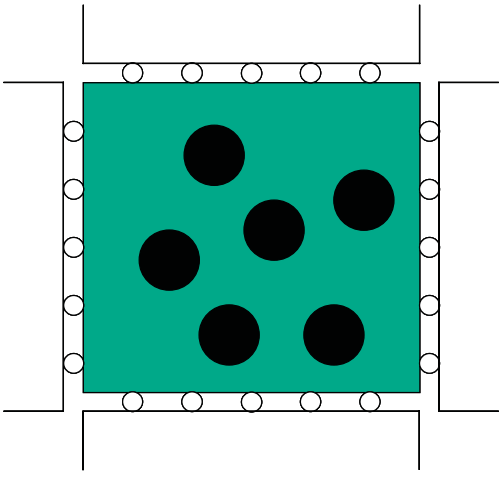

Fig. 3. Possible loading under the orthogonal-mixed boundary condition (2.13).

2.3. Apparent properties

In general, if we consider a body $B_\delta(\omega)$ of volume V subjected to a volume average strain by the boundary condition (2.11), i.e.

$$u_i(\mathbf{x}) = \varepsilon^0_{ij}x_j \qquad \forall\, \mathbf{x} \in \partial B_\delta, \tag{2.22}$$

given the continuity of displacements throughout, we have the average strain theorem

$$\bar{\varepsilon}_{ij} = \frac{1}{V}\int_V u_i n_j \mathrm{d}S = \frac{1}{V}\int_V \bar{\varepsilon}_{ik}x_k n_j \mathrm{d}S = \varepsilon^0_{ij}. \tag{2.23}$$

The apparent stiffness C^d_{klij} ($\equiv \mathbf{C}^d$) of $B_\delta(\omega)$ with a linear elastic microstructure may now be defined by

$$\bar{\sigma}_{ij} = C^d_{ijkl}\varepsilon^0_{kl}, \tag{2.24}$$

where $\bar{\sigma}$g is the volume average stress. Alternatively, we may consider the volume average energy density in $B_\delta(\omega)$

$$\begin{aligned}\bar{U} &= \frac{1}{2V}\int_V \sigma_{ij}\varepsilon_{ij}\mathrm{d}V = \frac{1}{2V}\int_{\partial V}\sigma_{ij}u_{i,j}dV \\ &= \frac{1}{2V}\int_{\partial V}\sigma_{ij}u_i n_j \mathrm{d}S = \frac{1}{2V}\int_V \sigma_{ij}\varepsilon^0_{ij}\mathrm{d}V = \frac{1}{2}\bar{\sigma}_{ij}\varepsilon^0_{ij} \\ &= \frac{1}{2}\varepsilon^0_{kl}C^d_{klij}\varepsilon^0_{ij},\end{aligned} \tag{2.25}$$

where the equilibrium $\sigma_{ij,j}=0$ was used. Thus, the apparent stiffness C^d_{klij} may be defined either from the mean stress $\bar{\sigma}$ or from the mean energy density $\bar{U}$ if the boundary condition (2.11) is imposed; see also [69].

On the other hand, considering the traction boundary condition (2.12), i.e.

$$t_i(\mathbf{x}) = \sigma^0_{ij} n_j(\mathbf{x}) \qquad \forall\, \mathbf{x} \in \partial B_\delta, \tag{2.26}$$

we first have the average stress theorem

$$\bar{\sigma}_{ij} = \frac{1}{V}\int_V \sigma_{ij}\mathrm{d}V = \frac{1}{V}\int_V \sigma^0_{ik} x_k n_j \mathrm{d}S = \sigma^0_{ij}. \tag{2.27}$$

We can now define the apparent compliance $\mathbf{S}^t$ from this relation

$$\bar{\varepsilon}_{ij} = S^t_{ijkl}\sigma^0_{ij}, \tag{2.28}$$

or from the volume average energy density in $B_\delta(\omega)$

$$\begin{aligned}\bar{U} &= \frac{1}{2V}\int_V \sigma_{ij}\varepsilon_{ij}\mathrm{d}V = \frac{1}{2V}\int_{\partial V} \sigma_{ij}u_{i,j}\mathrm{d}V \\ &= \frac{1}{2V}\int_{\partial V} \sigma_{ij}u_i n_j \mathrm{d}S = \frac{1}{2V}\int_V \sigma^0_{ij}u_{i,j}\mathrm{d}S = \frac{1}{2}\sigma^0_{ij}\bar{\varepsilon}_{ij} \\ &= \frac{1}{2}\sigma^0_{kl}S^t_{klij}\sigma^0_{ij}.\end{aligned} \tag{2.29}$$

This shows that the apparent compliance S^t_{klij} may be defined either from $\bar{\varepsilon}$ or from $\bar{U}$ if the boundary condition (2.12) is imposed; see also [23–25].

3. Spatial statistics

3.1. Stationarity of spatial statistics

In the following we revisit the key concepts of spatial homogeneity (stationarity) and ergodicity from the standpoint of what is required by Hill's definition of RVE. We shall do this in terms of a material property (or a vector of properties) Θ entering the heterogeneous medium model as a random field over the D-dimensional physical space

$$\Theta : \Omega \times \mathbb{R}^D \to \mathbb{R}. \tag{3.1}$$

In the case of an r-phase material microstructure, Θ is itself described by a random indicator function χ_r of all the phases. All that follows can then be generalized to a vector or tensor random field $\boldsymbol{\Theta}$, as may be the case with a linear elastic microstructure represented by a random stiffness field $\mathbf{C}$. Now, let us recall two well-known classes of spatial homogeneity:

Strict-sense stationary (SSS) random fields. This requires that all n-order probability distributions F_n are invariant with respect to arbitrary shifts $\mathbf{x}'$, and for any n and any choice of $\mathbf{x}_i$'s, they satisfy

$$\begin{aligned}&F_n(\theta_1, \ldots, \theta_n; \mathbf{x}_1, \ldots, \mathbf{x}_n) \\ &\quad = F_n(\theta_1, \ldots, \theta_n; \mathbf{x}_1 + \mathbf{x}', \ldots, \mathbf{x}_n + \mathbf{x}').\end{aligned} \tag{3.2}$$

Wide-sense (or weak-sense) stationary (WSS) random fields. The ensemble mean is constant and its finite-valued covariance depends only on the shift $\mathbf{h}$ from $\mathbf{x}$ to $\mathbf{x}+\mathbf{h}$

$$\begin{aligned}&\langle \Theta(\mathbf{x})\rangle \equiv \mu, \\ &\langle [\Theta(\mathbf{x}) - \langle\Theta(\mathbf{x})\rangle][\Theta(\mathbf{x}+\mathbf{h}) - \langle\Theta(\mathbf{x}+\mathbf{h})\rangle]\rangle \\ &\quad \equiv K_\Theta(\mathbf{h}) < \infty.\end{aligned} \tag{3.3}$$

Clearly, SSS implies WSS whenever the first-order distribution F_1 yields a finite second moment. It is through the covariance function $K_\Theta(\mathbf{h})$ that we introduce the concept of correlation distance l_c, which, in turn, gives an indication of decay of correlations between two different points. If this decay is such that $\Theta(\mathbf{x})$ and $\Theta(\mathbf{x}+\mathbf{h})$ become asymptotically uncorrelated according to $\lim_{|\mathbf{h}|\to\infty} K_\Theta(\mathbf{h})$, then, using l_c we would rewrite the separation of scales (1.1) as

$$\left.\begin{matrix} l_c < \\ l_c \ll \end{matrix}\right\} L \ll L_{\mathrm{macro}}. \tag{3.4}$$

In other words, the RVE of size $L = V^{1/D}$ ($D = 1,\ldots,3$) should be at least larger than l_c, and the material could be taken as homogeneous beyond L. This concept can also be applied to the SSS fields.

There also exist two more general classes of spatially homogeneous fields:

- intrinsically stationary (locally homogeneous) random fields,
- quasi-stationary random fields.

These types of random fields become relevant when there is no hope of establishing even the WSS property. In those situations, there is no hope of having the RVE in the sense employed in this paper, and the SVE is needed. In this paper we confine our attention to fields which have the SSS or WSS property.

3.2. Ergodicity of spatial statistics

Theoretical considerations. To estimate any random field of material properties via observations on a specific sample $\Theta(\omega)$, one needs some type of ergodic concept and/or ergodic assumption. First, recall that the classical ergodic property having its origin in dynamical systems of statistical physics is concerned with the random process parametrized by time t wandering almost surely through the entire space Ω. This means that a sample average converges

$$\overline{\Theta(\omega)} \equiv \lim_{T\to\infty}\frac{1}{T}\int_V \Theta(\omega, t)\mathrm{d}t. \tag{3.5}$$

The issue of actual convergence—i.e. the mathematical existence of the limit (3.5)—is the subject of Birkhoff's theorem, according to which Θ must be SSS and $\langle\Theta(t)\rangle = \mu$ must be finite. In general, however, $\overline{\Theta(\omega)}$ is a random variable, and of interest is finding conditions under which it equals the constant ensemble average

$$\overline{\Theta(\omega)} = \langle\Theta(t)\rangle. \tag{3.6}$$

The above is the basis of the engineering concept of the ergodic property, a quite different issue from the classical one above. In general, the 'engineering' *ergodicity* focuses on the question: Under what conditions do statistics in the form of time averages equal ensemble averages? Recall from probability theory that, one may establish ergodicity with respect to a certain parameter and in a certain sense (e.g. in quadratic mean), but this does not necessarily guarantee ergodicity with respect to another parameter.

When transcribed from a temporal process to a spatial one in one dimension, (3.6) takes the form

$$\overline{\Theta(\omega)} = \langle \Theta(x) \rangle. \tag{3.7}$$

Thus, for a random field, the spatial average involves measurements on a ray in a given direction x, whereby the volume $V=L$.

Perhaps the most basic result is that

$$\lim_{V\to\infty} \frac{1}{V} \int_V \Theta(\omega, x) \mathrm{d}x = \mu \tag{3.8}$$

is equivalent to

$$\begin{aligned} &\lim_{V\to\infty} \frac{1}{V} \int_V \langle \Theta(\omega, x) \rangle \mathrm{d}x = \mu \quad \text{and} \\ &\lim_{V\to\infty} \frac{1}{V^2} \int_V \int_V K_\Theta(x_1, x_2) \mathrm{d}x_1 \mathrm{d}x_2 = 0. \end{aligned} \tag{3.9}$$

Note that this does not require Θ to be even weak-sense stationary (!), and so this result may be used for intrinsically stationary and quasi-stationary random fields. In those cases, ergodicity is replaced by *local-ergodicity* and *quasi-ergodicity*. For example, the quasi-ergodic random field would require spatial averaging over domains smaller than l_c but larger than L_Θ.

When a WSS property is introduced, $K_\Theta(x_1, x_2) = K_\Theta(h)$, $h = |x_1 - x_2|$ and $(3.9)_2$ is replaced by

$$\lim_{V\to\infty} \frac{1}{V} \int_V \left(1 - \frac{x}{V}\right) K_\Theta(h) \mathrm{d}x = 0. \tag{3.10}$$

This, in turn, is assured providing

$$\lim_{|x|\to\infty} K_\Theta(x) = 0. \tag{3.11}$$

It follows that to estimate the mean (i.e. a first-order statistic) the covariance (i.e. a second-order statistic) is needed. This suggests a pattern revealed upon consideration of a condition for estimation of the covariance function itself from a single realization $\Theta(\omega)$. Namely, to ensure

$$\lim_{V\to\infty} \frac{1}{V} \int_V \Theta(\omega, x+h) \Theta(\omega, x) \mathrm{d}x = K_\Theta(h), \tag{3.12}$$

we need fourth-order moments, for any h_0,

$$\lim_{V\to\infty} \frac{1}{V} \int_V \left(1 - \frac{h}{V}\right) [K_\Theta^2(h) + K_\Theta(h+h_0) K_\Theta(h-h_0)] \mathrm{d}x = 0. \tag{3.13}$$

Measurements on finite domains. The above holds only with some accuracy, and the limiting process $V\to\infty$ cannot truly be carried out. In practice, the left and right hand sides of (3.7) are replaced by a spatial (or volume) average from a finite number of sampling points n taken over one realization on a finite domain (!)

$$\overline{\Theta(\omega)} \equiv \frac{1}{M} \sum_{m=1}^{M} \Theta(\omega, x_m), \tag{3.14}$$

and an ensemble average from a finite number of realizations ω taken at one sampling point

$$\langle \Theta(x) \rangle \equiv \frac{1}{N} \sum_{n=1}^{N} \Theta(\omega_n, x). \tag{3.15}$$

The fundamental question therefore is: What size V of the domain is large enough to attain the limits such as in (3.9) with a certain precision? A closely related issue is the actual choice between $l_c < L$ and $l_c = L$ in the separation of scales (1.1). Quantitative answers can be found with the help of mechanics problems elaborated in Sections 4 and 5 below.

Ergodic response. Any given boundary value problem for an elastic body $\mathcal{B} = \{B(\omega); \omega \in \Omega\}$ is defined by the equilibrium Eq. (1.8), Hooke's law, compatibility conditions, and some boundary conditions. Now, subject $B(\omega)$ to a uniform boundary condition such as (2.11) or (2.12) and find the ensemble of solutions

$$\{\varepsilon(\omega, \mathbf{x}),\ \sigma(\omega, \mathbf{x}), \mathbf{u}(\omega, \mathbf{x});\ \omega \in \Omega,\ \mathbf{x} \in V\}, \tag{3.16}$$

which would represent a complete solution of the stochastic mechanics problem. Then, at any point $\mathbf{x}$, we may define effective moduli $\mathbf{C}^{\mathrm{eff}}(\mathbf{x})$ as

$$\langle \sigma(\mathbf{x}) \rangle = \langle \mathbf{C}(\mathbf{x}) : \varepsilon(\mathbf{x}) \rangle = \mathbf{C}^{\mathrm{eff}}(\mathbf{x}) : \langle \varepsilon(\mathbf{x}) \rangle. \tag{3.17}$$

Note:

(i) For any given boundary conditions, $\mathbf{C}^{\mathrm{eff}}$ is, in general, a function of $\mathbf{x}$.
(ii) $\mathbf{C}^{\mathrm{eff}}$ also generally depends on the boundary conditions applied.
(iii) Assuming $\mathcal{B}$ is ergodic in the sense that the field $\mathbf{C}$ is ergodic, the explicit dependence on location in (3.17) vanishes and we can write

$$\langle \varepsilon(\mathbf{x}) \rangle = \bar{\varepsilon} \quad \text{or} \quad \langle \sigma(\mathbf{x}) \rangle = \bar{\sigma}, \tag{3.18}$$

providing (2.11), respectively (2.12), is applied and the displacement and stress fields are continuous; consequently,

$$\bar{\sigma} = \mathbf{C}^{\text{eff}} : \bar{\varepsilon}. \tag{3.19}$$

(iv) Providing $\mathcal{B}$ is ergodic in the sense that the field $\mathbf{C}$ is ergodic, and mesoscale windows tend to macroscale $\delta \to \infty$, write the Hill condition (2.8) as

$$\langle \varepsilon : \sigma \rangle = \langle \varepsilon \rangle : \langle \sigma \rangle. \tag{3.20}$$

Of course, by analogy to (2.9), we have

$$\langle \varepsilon' : \sigma' \rangle = 0, \tag{3.21}$$

which means that stresses and strains are statistically uncorrelated.

4. Hierarchies of mesoscale bounds for linear elastic microstructures

4.1. Basic results

We first sketch the proof of a hierarchy of bounds on the macroscopically effective stiffness tensor $\mathbf{C}^{\text{eff}}$, i.e. the RVE's response. We take a square-shaped 2D (or a cubic-shaped 3D) body $B_\delta(\omega)$ to be described everywhere by the local stress–strain relations $\boldsymbol{\sigma} = \boldsymbol{C}(\omega, \mathbf{x}):\boldsymbol{\varepsilon}$. We call (2.11) an *unrestricted uniform displacement boundary condition*. We also define a *restricted displacement boundary condition*

$$\mathbf{u}^r(\mathbf{x}) = \varepsilon^0 : \mathbf{x} \qquad \forall\, \mathbf{x} \in \partial B_{\delta_s} \qquad s = 1, \ldots, 4, \tag{4.1}$$

acting on a partition of $B_\delta(\omega)$ into four square-shaped subdomains B_{δ_s} such that $B_\delta = \cup_{s=1}^4 B_{\delta_s}$. In 3D the partition involves eight domains, but we work in 2D for the sake of clarity. The superscript r in Eq. (4.1) indicates a 'restriction'.

We recall the minimum potential energy principle for the fields $(\tilde{\sigma}, \tilde{\varepsilon})$ in $B_\delta(\omega)$ (e.g. [28])

$$\int\limits_{\partial B_\delta^t} \mathbf{t}\cdot\tilde{\boldsymbol{u}}\,\mathrm{d}S - \frac{1}{2}\int\limits_{B_\delta} \tilde{\boldsymbol{\sigma}} : \tilde{\varepsilon}\,\mathrm{d}V \le \int\limits_{\partial B_\delta^t} \mathbf{t}\cdot\mathbf{u}\,\mathrm{d}S - \frac{1}{2}\int\limits_{B_\delta} \sigma : \varepsilon\,\mathrm{d}V, \tag{4.2}$$

where the tilde indicates kinematically admissible fields. This allows us to prove that the solution fields $(\tilde{\sigma}^r, \tilde{\varepsilon}^r)$ under the restricted condition (4.1) are admissible with respect to the unrestricted condition (2.11) (but not vice versa), so that

$$\overline{\sigma\varepsilon} \le \tilde{\sigma}^r \tilde{\varepsilon}^r. \tag{4.3}$$

This in turn implies a weak inequality between the mesoscale stiffness tensors obtained under unrestricted $(\mathbf{C}_\delta^d(\omega))$ and restricted $(\mathbf{C}_\delta^{dr}(\omega))$ conditions

$$\mathbf{C}_\delta^d(\omega) \le \mathbf{C}_\delta^{dr}(\omega) = \frac{1}{4}\sum_{s=1}^{4} \mathbf{C}_{\delta_s}^d(\omega) \qquad \forall\, \delta' = \delta/2. \tag{4.4}$$

That is, the effective stiffness of a partitioned domain subjected to (4.1) involves respective stiffnesses of four subdomains. Now, in view of the tacitly assumed statistical homogeneity and ergodicity of the material, ensemble averaging of (4.4) allows us to replace $\mathbf{C}_\delta^d(\omega)$ by $\langle \mathbf{C}_\delta^d \rangle$, and $\mathbf{C}_\delta^{dr}(\omega)$, by $\langle \mathbf{C}_{\delta'}^d \rangle$, so that

$$\langle \mathbf{C}_\delta^d \rangle \le \langle \mathbf{C}_{\delta'}^d \rangle \qquad \forall\, \delta' = \delta/2. \tag{4.5}$$

By applying this inequality to ever larger windows *ad infinitum* we get a hierarchy of bounds on $\langle \mathbf{C}_\infty^d \rangle$ from above

$$\langle \mathbf{C}_\infty^d \rangle \le \cdots \le \langle \mathbf{C}_\delta^d \rangle \le \langle \mathbf{C}_{\delta'}^d \rangle \le \cdots \le \langle \mathbf{C}_1^d \rangle \equiv \mathbf{C}^V \qquad \forall \delta' = \delta/2. \tag{4.6}$$

In fact, we have

$$\langle \mathbf{C}_\infty^d \rangle = \mathbf{C}_\infty^{\text{eff}} = \mathbf{C}^{\text{eff}} \tag{4.7}$$

for the macroscopically effective response $(\delta \to \infty)$ because, by the ergodicity argument, it must be deterministic. On the upper end, the hierarchy stops at the scale of a single heterogeneity. Now, since the single heterogeneity—like an inclusion or a crystal—is homogeneous, the uniform strain is true strain, so that ensemble averaging gives the Voigt bound $\mathbf{C}^{\text{V}}$.

The above derivation suggests an analogous procedure for proving a hierarchy bounding the effective stiffness $\mathbf{C}^{\text{eff}}(\equiv(\mathbf{S}^{\text{eff}})^{-1}$ or the effective compliance) from below. The proof is analogous, providing we first replace the displacement by traction boundary conditions (2.12) and use the minimum complementary energy principle for statically admissible fields $(\tilde{\sigma}, \tilde{\varepsilon})$ in $B_\delta(\omega)$

$$\frac{1}{2}\int\limits_{B_\delta} \sigma : \varepsilon\,\mathrm{d}V - \int\limits_{\partial B_\delta^u} \mathbf{t}\cdot\mathbf{u}\,\mathrm{d}S \le \frac{1}{2}\int\limits_{B_\delta} \tilde{\sigma} : \tilde{\varepsilon}\,\mathrm{d}V - \int\limits_{\partial B_\delta^u} \tilde{\mathbf{t}}\cdot\mathbf{u}\,\mathrm{d}S. \tag{4.8}$$

Using the Hill condition and ensemble averaging, leads then to

$$\left\langle \mathbf{S}_\delta^t \right\rangle \le \left\langle \mathbf{S}_{\delta'}^t \right\rangle \quad \forall\, \delta' = \delta/2. \tag{4.9}$$

By applying this inequality to ever larger windows *ad infinitum* we get a hierarchy of bounds on $\langle \mathbf{S}_\infty^t \rangle$ from above (i.e. on $\left\langle \mathbf{C}_\infty^d \right\rangle$ from below)

$$\left\langle \mathbf{S}_\infty^t \right\rangle \le \cdots \le \left\langle \mathbf{S}_\delta^t \right\rangle \le \left\langle \mathbf{S}_{\delta'}^t \right\rangle \le \cdots \le \left\langle \mathbf{S}^t \right\rangle \equiv S^R \qquad \forall \delta' = \delta/2, \tag{4.10}$$

where

$$\left\langle \mathbf{S}_\infty^t \right\rangle = \mathbf{S}_\infty^{\text{eff}} = \mathbf{S}^{\text{eff}} = (\mathbf{C}^{\text{eff}})^{-1}. \tag{4.11}$$

Combining relations (4.6) with (4.10), we arrive at a scale-dependent hierarchy of bounds on the macroscopically effective moduli

$$\left\langle \mathbf{S}^t \right\rangle^{-1} \le \cdots \le \left\langle \mathbf{S}_{\delta'}^t \right\rangle^{-1} \le \left\langle \mathbf{S}_\delta^t \right\rangle^{-1} \le \cdots \le \mathbf{C}_\infty^{\text{eff}} \le \cdots \le \left\langle \mathbf{C}_\delta^d \right\rangle \le \left\langle \mathbf{C}_{\delta'}^d \right\rangle \le \cdots \le \left\langle \mathbf{C}^d \right\rangle \qquad \forall \delta' = \delta/2. \tag{4.12}$$

These hierarchies were first derived by Huet [13]. A more rigorous proof using techniques of homogenization and probability theories was given by Sab [15], see Section 4.2 below. The decrease of the upper (displacement-controlled) bound with increasing scale appears to had first been demonstrated on planar random networks of Delaunay topology by Ostoja-Starzewski and Wang [29] the uniform traction conditions, however, could not be applied in a unique way to such a disordered discrete system, see also [30].

Spatial statistics aspects. Considering that the hierarchy (4.12) is stated in terms of the ensemble averages, it suffices to choose the setting of material properties specified via wide-sense stationary random fields. Furthermore, note that in the case of $\mathbf{C}$ being an isotropic random field, $\mathbf{C}^{\text{eff}}$ should become an isotropic tensor involving two Lamé constants λ^{eff} and μ^{eff}. On the other hand, for an orthotropic random field $\mathbf{C}$, $\mathbf{C}^{\text{eff}}$ should become an orthotropic tensor.

The hierarchy (4.12) has been shown to hold for commensurate partitions on mesoscale, i.e. $\delta' = \delta/2$. An extension of these inequalities to arbitrary pairs of mesoscales $\delta < \delta$ is also true [31].

4.2. Homogenization theory viewpoint

We assume the composite—such as that of Fig. 2—to be made of a finite number of r phases each of which is linear elastic and elliptic: $0 < \mathbf{e}{:}\mathbf{C}{:}\mathbf{e} < \infty$, $\forall\, \mathbf{e} \neq \mathbf{0}$. Next, following Sab [15], let $F(B, \boldsymbol{\Theta})$ represent a real functional of the open bounded domain B of volume V and random field $\boldsymbol{\Theta}$ with the following five properties:

1. F is a property of the medium invariant with respect to any translation in the material domain.
2. F or any partition of the domain B into n disjoint subdomains, F satisfies a subadditivity property

$$F(B,\Theta) \leq \sum_{i=1}^{n} \frac{V_i}{V} F(B_i,\Theta) \quad B = \cup_{i=1}^{n} B_i. \tag{4.13}$$

3. F is a measurable mapping with respect to the sample space Ω of outcomes ω.
4. $\boldsymbol{\Theta}$ is a statistically homogeneous, ergodic random field.
5. F is uniformly bounded in B and ω in the sense that there exists a real b, such that

$$|F(B,\Theta)| \leq 0 \quad \forall\, B, \omega. \tag{4.14}$$

Let us now take B to be a square-shaped domain, with side of length L, and which contains some microstructure of characteristic microscale d, see, e.g. Fig. 2. With the conditions 1–5 satisfied, we can adopt the result that there exists a non-random (i.e. deterministic) constant F^{hom} such that, for all ω with probability one, we will have

$$\lim_{L/d\to\infty} |F(B,\Theta)| = F^{\text{hom}} \quad \forall\, B, \omega. \tag{4.15}$$

with the bound

$$\inf_{L/d} (F(B,\Theta)) = F^{\text{hom}} \quad \forall\, B, \omega. \tag{4.16}$$

This limit is understood in the sense of the homogenization theory: $\mathbf{x} \to F^{\varepsilon}(\mathbf{x}) = F(\mathbf{x}/\varepsilon) \equiv F^{\varepsilon}(\mathbf{y})$, where, $\mathbf{x}$ and $\mathbf{y}$ are the so-called slow (macroscopic) and fast (microscopic) variables, respectively, and ε is a small parameter, reciprocal of our $\delta = L/d$. The limit $\delta \to \infty$ should be taken here in such a way that L is kept finite so as to keep the energy finite. If F represents the volume average elastic energy density (or complementary) energy density, then, $\boldsymbol{\Theta}$ stands for the stiffness $\mathbf{C}$ (respectively, compliance $\mathbf{S}$) tensor of the domain B, and from (4.16) one has

$$\sup_{L/d} \langle \mathbf{S} \rangle^{-1} = (\mathbf{S}^{\text{hom}})^{-1} = \mathbf{C}^{\text{hom}} = \inf_{L/d} \langle \mathbf{S} \rangle. \tag{4.17}$$

where $(\mathbf{S}^{\text{hom}})^{-1} = \mathbf{C}^{\text{hom}}$ is the macroscopic (effective) stiffness tensor $\mathbf{C}^{\text{eff}}$ in the sense of Hill [1]. However, (4.17) does not assert that the averages $\langle \mathbf{S} \rangle^{-1}$ and $\langle \mathbf{C} \rangle$ are monotonic functions of L/d $(= \delta)$; this property, resulting in a scale-dependent hierarchy of the apparent properties convergent to $\mathbf{C}^{\text{hom}}$ was obtained above, following a procedure originally due to Huet [13]; see also [32,33].

Finally we note that, for the RVE $B_{\delta\to\infty}(\omega)$, in the notation of homogenization theory, we have

$$\Sigma(\omega) = \bar{\sigma}_{\delta\to\infty}(\omega) \quad \mathbf{E}(\omega) = \bar{\varepsilon}_{\delta\to\infty}(\omega). \tag{4.18}$$

4.3. Apparent moduli in in-plane elasticity

When considering the apparent constitutive law

$$\sigma_{ij} = C_{ijkl}(\omega, \mathbf{x}) \varepsilon_{kl} \quad i,j,k,l = 1,2, \tag{4.19}$$

of a planar elastic material $B_{\delta}(\omega)$, we must, in general, deal with an arbitrary anisotropy. Thus, to determine six unknown C^{d}_{ijkl}'s (or S^{t}_{ijkl}'s) for $B_{\delta}(\omega)$ we need six tests, Fig. 4. When seeking C^{d}_{ijkl}'s, each test is run by applying the affine displacements on B so that the strain energy density is

$$\begin{aligned} U_{\delta} = \frac{V}{2} \bar{\sigma}_{ij} \varepsilon^{0}_{ij} = \frac{V}{2} \varepsilon^{0}_{ij} C_{ijkl} \varepsilon^{0}_{kl} = \frac{V}{2} \Big[& C_{1111} \left(\varepsilon^{0}_{11}\right)^2 + C_{2222} \left(\varepsilon^{0}_{22}\right)^2 \\ & + C_{1212} \left(\varepsilon^{0}_{12}\right)^2 + 2\varepsilon^{0}_{11} C_{1122} \varepsilon^{0}_{22} + 2\varepsilon^{0}_{22} C_{2212} \varepsilon^{0}_{12} \\ & + 2\varepsilon^{0}_{12} C_{1211} \varepsilon^{0}_{11} \Big]. \end{aligned} \tag{4.20}$$

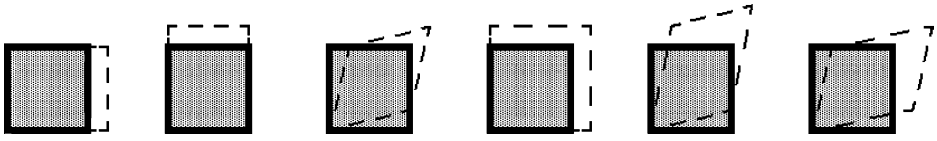

Fig. 4. Six tests—#1, #2,…,#6 from left to right—to determine the six unknowns of the in-plane stiffness tensor C_{ijkl}.

In each and every test, separately, the energy is found by computational mechanics, and this is set equal to a corresponding special form of (4.20). For example, in test #1,

$$U_\delta = \frac{V}{2} C_{1111} \left(\varepsilon_{11}^0\right)^2, \tag{4.21}$$

from which we infer C_{1111}. Similarly, from the test #2 we find C_{2222}, while test #3 gives C_{1211}. We are then in a position to find C_{1122} from

$$U_\delta = \frac{V}{2}\left[C_{1111}\left(\varepsilon_{11}^0\right)^2 + C_{2222}\left(\varepsilon_{22}^0\right)^2 + 2\varepsilon_{11}^0 C_{1122}\varepsilon_{22}^0\right], \tag{4.22}$$

and then C_{2212} as well as C_{1211} in an analogous fashion.

In practice, one can proceed by truly carrying out six tests, or by carrying out only the three tests #1–#3 of Fig. 4, and then combining their results through a superposition. In any case, the solution necessarily involves some computational mechanics method for discretization of the composite, such as spring networks, finite elements, or boundary elements.

In the case of traction boundary conditions, determination of the apparent compliances follows the same type of approach and one works with the complementary energy, that is

$$\begin{aligned} U_\delta^* = \frac{V}{2}\sigma_{ij}^0 \bar{\varepsilon}_{ij} = \frac{V}{2}\sigma_{ij}^0 S_{ijkl}\sigma_{kl}^0 = \frac{V}{2}\Big[S_{1111}\left(\sigma_{11}^0\right)^2 + S_{2222}\left(\sigma_{22}^0\right)^2 \\ + S_{1212}\left(\sigma_{12}^0\right)^2 + 2\sigma_{11}^0 S_{1122}^0 \sigma_{22}^0 + 2\sigma_{22}^0 S_{2212}^0 \sigma_{12}^0 \\ + 2\sigma_{12}^0 S_{1211}^0 \sigma_{12}^0\Big]. \end{aligned} \tag{4.23}$$

An extension of this methodology to three dimensions is straightforward. Examples of bounds obtained in this way are given in [35,41].

4.4. Examples of hierarchies of mesoscale bounds

4.4.1. Random chessboards and Bernoulli lattices

In this section we focus on anti-plane elasticity of random microstructures, which, by virtue of mathematical analogies recalled in Appendix, also gives information on various other physical problems of material systems having the same morhpology. Let us now consider the Bernoulli lattice process $\Phi_{p,a}$ on a Cartesian lattice of spacing a with each point of this lattice being of type 1 (or 2) with probability p (respectively, $q=1-p$) independently of all the other points. Evidently, p and q define the volume fractions of both types of phases (1 and 2). Clearly, the local stress and strain concentrations cannot be resolved, but the statistics of such a simple system gives an indication of the statistics of random media because this, perhaps, is the simplest setup in which to investigate the scale and volume fraction dependence of the ensemble average estimates based on the essential (e) and natural (n) boundary conditions. The notation e and n is equivalent to d and t, respectively. In three Fig. 5(a–c) taken from [34] we give traces of $\left\langle \mathbf{C}_\delta^e \right\rangle$ and $\left\langle \mathbf{S}_\delta^n \right\rangle^{-1}$ at $\delta=4$, 10, and 20 (for the highest contrast) and their comparison with Hashin (-Shtrikman) upper and lower bounds

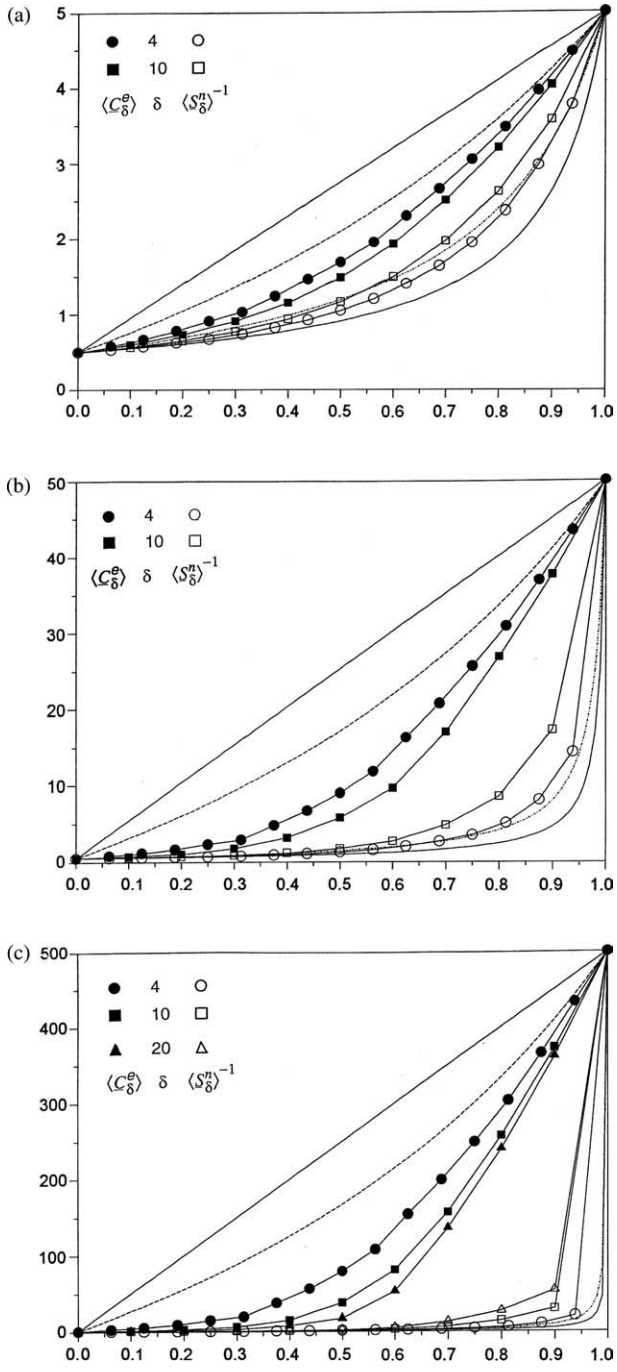

Fig. 5. Mesoscale bounds on $tr(\mathbf{C}^{\text{eff}})$ for a random disk-matrix at contrasts 10 (a), 100 (b), and 1000 (c), showing $\langle tr\mathbf{C}_\delta^e \rangle$ and $\langle tr\mathbf{S}_\delta^n \rangle^{-1}$ at $\delta=4$, 10 and 20; also shown, by dashed lines, are Hashin bounds C_u^H and C_l^H; after [34].

$$\begin{aligned} C_u^H &= C_2 + f_1[1/(C_1 - C_2) + f_2/2C_2]^{-1} \\ C_l^H &= C_1 + f_2[1/(C_2 - C_1) + f_1/2C_1]^{-1}. \end{aligned} \tag{4.24}$$

Observe that C_u^H and C_l^H are outside the windows of size 4. In other words, relatively very small windows can give tighter mesoscale bounds than those of Hashin.

Note that the problem of scale dependence, especially in the setting of such binary systems, is akin to the so-called *finite-size scaling* in statistical physics, but the attention in that area

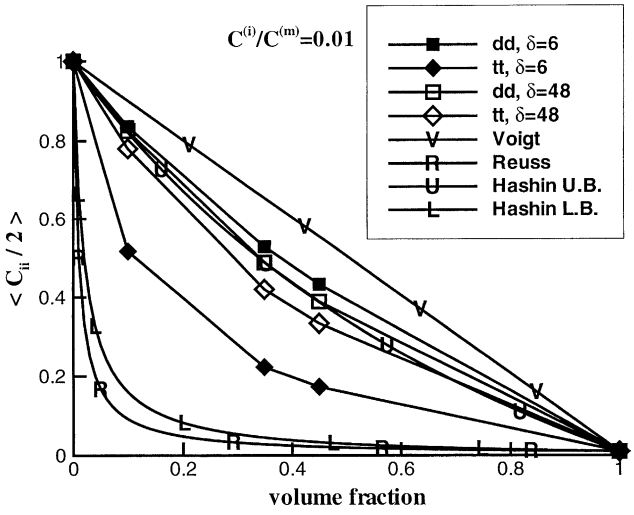

Fig. 6. Bounds for a random disk-matrix composite at contrast $C^{(i)}/C^{(m)}=0.01$, showing mesoscale bounds under uniform displacement (*dd*) and traction (*tt*) boundary conditions on mesoscales $\delta=6$ and 48, as well as the Voigt, Reuss, and Hashin(-Shtrikman) upper and lower bounds; after [41].

has always been focused on the phase transition problems [36]. The approach to such a transition at about 2/3 volume fraction of the soft phase is shown in the last of three figures here—at contrast 1000. However, in contradistinction to the terminology of phase transitions, we now have a different tool to describe the scale dependence. The particular case of $p=q=0.5$ has been studied in [34], and it was found that

$$\mathbf{C}_\delta^e = \exp[-\delta^{-m}] \quad \mathbf{S}_\delta^n = \exp[\delta^{-n}], \tag{4.25}$$

where m and n are functions of the contrast α

$$m = 3.8\alpha^{0.14} \quad n = 2.4\alpha^{0.59}. \tag{4.26}$$

These results were obtained from computations over a range of scales 1–1000. While the smallest scale can be calculated explicitly as the Voigt and Reuss bounds, the largest involved a lattice of 1000×1000 nodes, i.e. having 10^6 degrees of freedom. The parameter space of contrast and volume fraction is vast, and therefore only select cases can be run numerically at these large scales. But, (4.25)–(4.26) give an idea of the scaling laws for other volume fractions.

Now, the Bernoulli lattice at volume fraction below, say, 30% can also be interpreted as a very crude model of a disk matrix composite—again with one degree of freedom per disk. Given the fact that a more realistic spring network model requires several (at least five) lattice spacings per disk, a lattice of some 5000×5000 nodes (25×10^6 degrees of freedom) would have to be run. Thus, the above scaling laws provide the best available indication of finite-size scaling of both bounds, $\mathbf{C}_\delta^e$ and $\mathbf{S}_\delta^n$, of disk-matrix composites.

4.4.2. Disk-matrix composites

The hierarchy of bounds (4.12) is now illustrated on the example of a planar disk-matrix composite [41]. These microstructures have been generated via the planar Poisson point process for disk centers, with sequential inhibition rule that prevents any two Poisson points from coming closer than 110% of diameter, so as to avoid the numerically and analytically difficult problem of very narrow necks between disks. First, in Fig. 6 (in analogy to Fig. 5 above) we give bounds stemming from uniform displacement and uniform traction boundary conditions for the entire range of volume fractions at contrast $C^{(i)}/C^{(m)}=10$ and mesoscales $\delta=6$ and 48. These results are compared to those of Voigt and Reuss bounds, as well as Hashin(-Shtrikman) upper and lower bounds e.g. [19]. To further illustrate the scaling trends of all the boundary conditions (2.11)–(2.16), in Fig. 7 we reproduce two graphs—at contrasts $C^{(i)}/C^{(m)}=10$ and $C^{(i)}/C^{(m)}=1000$, respectively—at volume fraction 35%. Clearly, the larger is the contrast in the composite, the larger is the mesoscale window necessary to attain the RVE within, say, 10%. The mixed boundary conditions give responses intermediate between those have purely kinematic and purely traction type. However, at high contrasts (Fig. 7(b)) their use tends to disappear.

We next compare responses of the disk-matrix composite with relatively hard disks versus one with relatively soft disks, both at volume fraction 20%. In the first case, we have a soft matrix ($C^{(m)}=1$) and inclusions $C^{(i)}=10^2$ in Fig. 8(a), and $C^{(i)}=10^4$ in Fig. 8(b). Clearly,

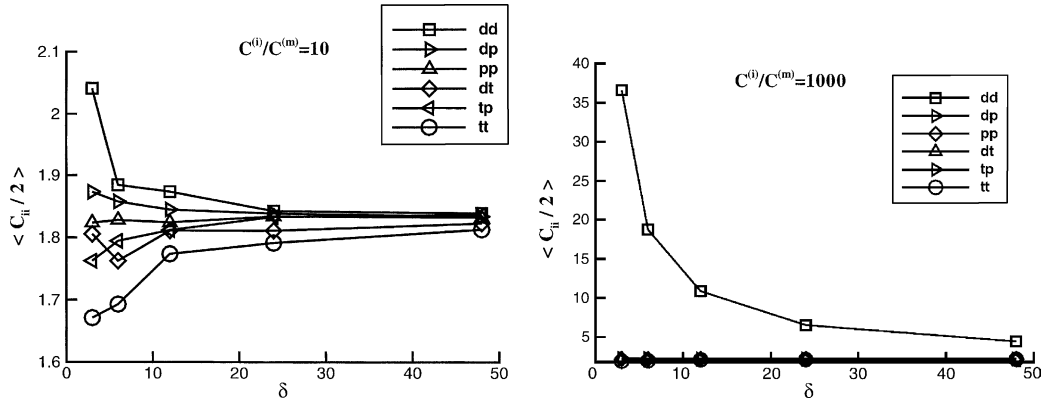

Fig. 7. Effect of boundary conditions in planar disk-matrix composites: displacement-controlled (dd), traction-controlled (tt), peri-odic (pp), and mixed (displacement-periodic (dp), displacement-traction (dt), and traction-peri-odic (tp)) on the half-trace of the apparent anti-plane stiffness tensor in function of the mesoscale d, at contrasts 10 (a) 1,000 (b).

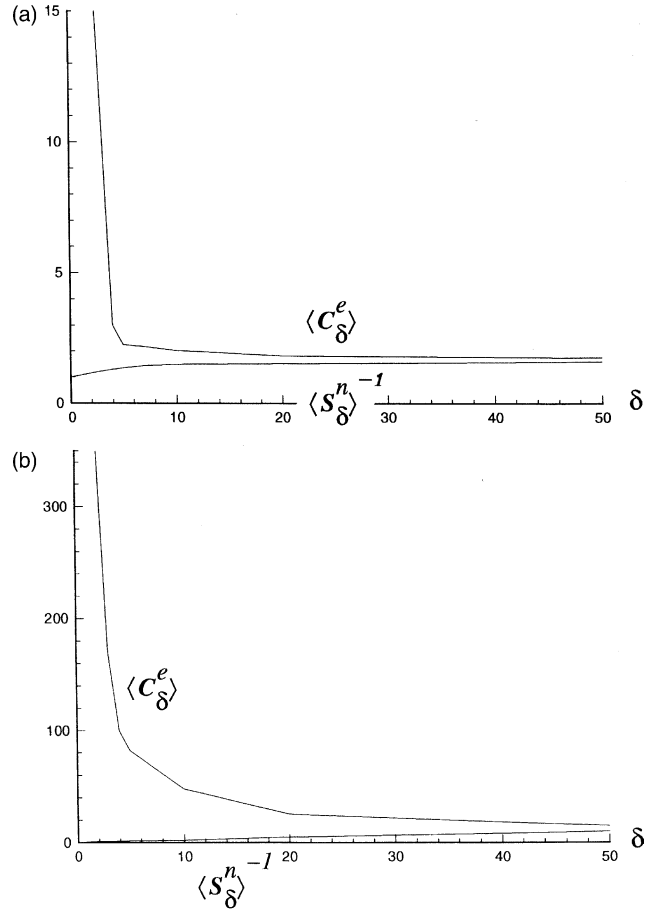

Fig. 8. A hierarchy of scale dependent bounds on $tr(\mathbf{C}^{\text{eff}})$ of the disk-matrix composite at contrasts 10^2 (a), and 10^4 (b); after [33].

the larger is the contrast in the composite, the larger is the mesoscale window necessary to attain the RVE within, say, 10%. Thus, to attain the discrepancy between $\langle \mathbf{S}_\delta^n \rangle^{-1}$ and $\langle \mathbf{C}_\delta^e \rangle$ of about 30% at contrast 10^2 on mesoscale $\delta = 10$, one has to take $\delta = 50$ at contrast 10^4.

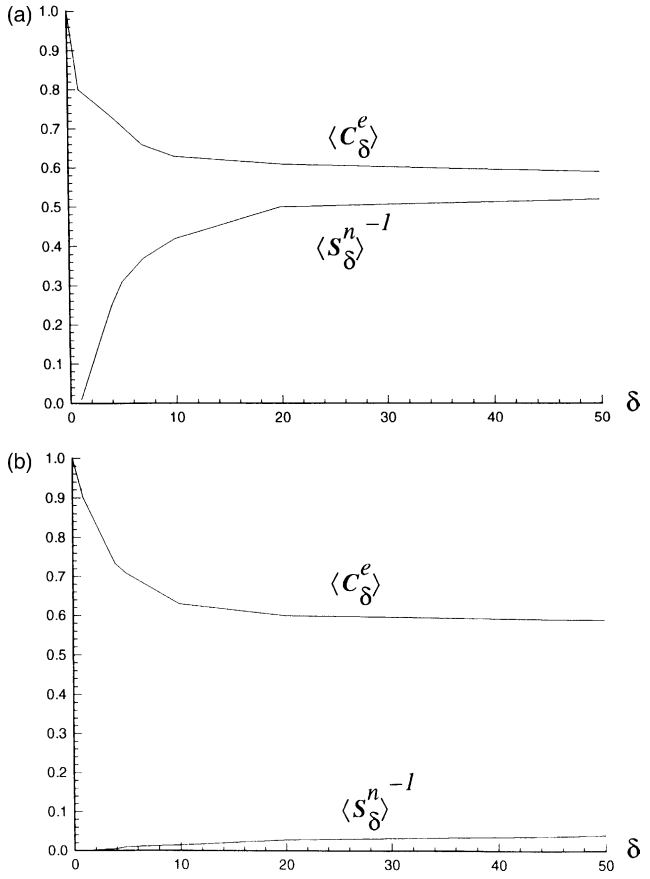

Fig. 9. A hierarchy of scale dependent bounds on $tr(\mathbf{C}^{\text{eff}})$ for the disk-matrix composite at contrasts 10^{-2} (a), and 10^{-4} (b); after [33].

In Fig. 9 we show results for the opposite case: soft inclusions in a hard matrix, with the same volume fraction 20%. Again, we consider two cases of contrast—$C^{(i)}/C^{(m)} = 10^{-2}$ and 10^{-4}—while keeping the matrix at $C^{(m)} = 1$. The first case of contrast is shown in Fig. 9(a), and the second one in Fig. 9(b). As before, an increase in the contrast in the composite has the effect of slowing

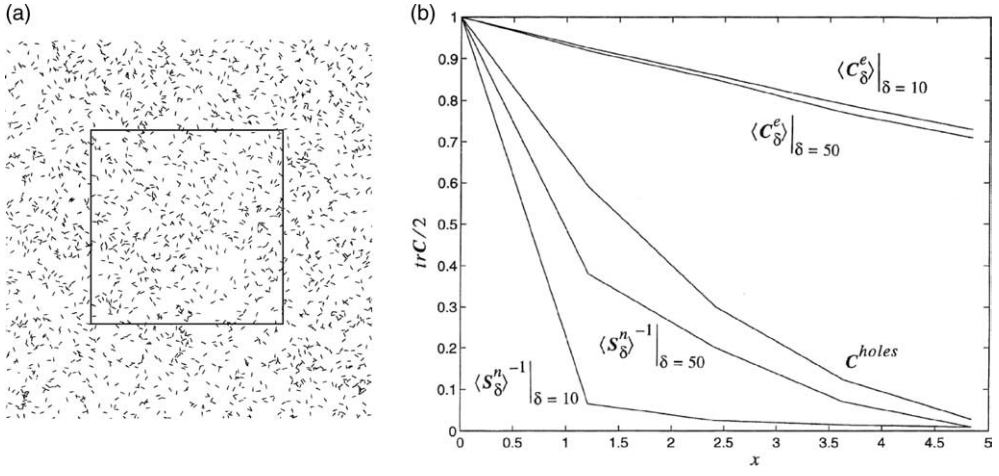

Fig. 10. (a) A 1000×1000 window of 2000 randomly placed 10×1 needles with an isotropic distribution; a subwindow of size ($\delta = 50$) is indicated. (b) Normalized overall moduli $\langle \mathbf{C}_\delta^e \rangle$ and $\langle \mathbf{S}_\delta^n \rangle^{-1}$, at $\delta = 10$ and $\delta = 50$, and the effective stiffness $\mathbf{C}^{\text{holes}}$ for a random field of short (1×10) needles (such as that of Fig. 13), as functions of the volume fraction x. Data were computed only at discrete intervals $x = 1.21$, 2.42, 3.63, and 4.84; after [31].

down the convergence of the product $\mathbf{S}_\delta^n : \mathbf{C}_\delta^e$ to unity with δ increasing, but, by comparison with Fig. 8, this convergence is relatively much slower (!) for extreme contrasts. It follows that one needs to go to very large scales in order to homogenize such a composite material. This is the principal difference from the case of high contrasts, and is indicative of all the material systems with soft inclusions of whatever shape. Both Figs. 8 and 9 were obtained using a spring network of a much finer scale than the single inclusion [37].

4.5. Needle and crack systems

Since we are interested in planar fields of randomly placed needles, we consider a random fiber field generated from the Poisson point process—Fig. 10(a) presents its typical realization $B(\omega)$ [31]. The process density chosen here is 0.015. As in the previous section, the material has two locally isotropic phases—matrix (m) and inclusions (i)—and we keep $C^{(m)}=1$ and vary $C^{(i)}$.

Before we proceed further, we note that work on effective moduli of materials with microcracks dates back to [38] and [39], while a comprehensive review was given by Kachanov [40]. The effective medium theory, however, cannot say anything about the finite-size scaling of (mesoscale) moduli and their statistics; nor is it reliable for higher crack densities. Note also that these problems—especially in connection with finite-size scaling—can be treated by the lattice, or spring-network models [37], bearing in mind two approximations: needles have a finite thickness, and the contrast is finite although it can be made very close to zero.

When studying scaling of $\langle \mathbf{C}_\delta^e \rangle$ and $\langle \mathbf{S}_\delta^n \rangle^{-1}$ for needle systems at contrasts 10^{-2} and 10^{-4}, we found the same type of slow approach to the RVE as that in soft disk-matrix systems noted in the preceding section. Now, in the studies of effective moduli of heterogeneous materials, the resulting $\mathbf{C}^{\text{eff}}$ is typically presented versus the volume fraction x of one of the phases. For a system of short needles, this is shown in Fig. 10(b) in terms of $\mathbf{C}^{\text{holes}}$ against $x = nL_{eff}^2$ almost all the way to the percolation point at ~ 5.9; $\mathbf{C}^{\text{holes}}$ is computed by the physicist's mean field method for needle-shaped holes of any aspect ratio and with arbitrarily strong interactions. In addition, we also plot here the Dirichlet and Neumann moduli and at two mesoscales: $\delta=10$ and $\delta=50$. To sum up, this figure displays (i) a very slow approach of $\langle \mathbf{C}_\delta^e \rangle$ and $\langle \mathbf{S}_\delta^n \rangle^{-1}$ to the RVE (i.e. curve $\mathbf{C}^{\text{holes}}$), and (ii) a discrepancy between $\mathbf{C}^{\text{holes}}$ and the Dirichlet as well as the Neumann bounds. Note that $\mathbf{C}^{\text{holes}}$ corresponds to an effective (macroscopic) response of a very large random system, that is typically computed under periodic boundary conditions, see also [42].

For the system at hand, there is an interesting result concerning the statistics of second invariants of $\mathbf{C}_\delta^e(\omega)$ and $\mathbf{S}_\delta^n(\omega)$. Namely, within a few percent, their coefficients of variation are constant for a given type of boundary conditions (either Dirichlet or Neumann), are independent of the changing mesoscale δ, and independent of the contrast in the material, except, of course the singular and trivial case of $C^{(m)}/C^{(i)}=1$ [41,43].

5. Hierarchies of mesoscale bounds for nonlinear elastic and/or inelastic materials

5.1. Nonlinear elastic materials

5.1.1. General

It should be clear from the derivation of mesoscale bounds for linear elastic materials that three properties are required:

(i) statistical homogeneity and ergodicity (strictly speaking, quasi-ergodicity);
(ii) Hill condition leading to admissible boundary conditions;
(iii) variational principle.

It follows that the mesoscale bounds can be shown to hold for other types of materials providing these three properties are appropriately generalized. In the following we present some principal results.

Consider physically nonlinear elastic materials in the range of infinitesimal strain, described by the constitutive law

$$\sigma = \sigma(\varepsilon) = \frac{\partial w(\varepsilon)}{\partial \varepsilon} \quad \varepsilon = \varepsilon(\sigma) = \frac{\partial w^*(\sigma)}{\partial \sigma}, \tag{5.1}$$

where the energy densities are related by $w^* = \sigma\cdot\varepsilon - w$; w is a statistically homogeneous and ergodic field. The Hill condition, and its implication for the type of admissible boundary conditions, is

$$\overline{\sigma : \mathrm{d}\varepsilon} = \bar{\sigma} : \overline{\mathrm{d}\varepsilon} \Leftrightarrow \int_{\partial B_\delta} (\mathbf{t} - \bar{\sigma}\cdot\mathbf{n})\cdot(\mathrm{d}\mathbf{u} - \overline{\mathrm{d}\varepsilon}\cdot\mathbf{x})\mathrm{d}S = 0, \tag{5.2}$$

where $\bar{\sigma} = \sigma^0$ and $\bar{\varepsilon} = \varepsilon^0$. This results in the same three types of boundary conditions on the mesoscale as in the linear elastic case. For a given realization $B_\delta(\omega)$ of the random medium B_δ on some mesoscale δ, the first of these yields an apparent constitutive law

$$\bar{\sigma} = \bar{\sigma}(\varepsilon^0). \tag{5.3}$$

Similarly, the traction condition results in an apparent constitutive law

$$\bar{\sigma} = \bar{\sigma}(\varepsilon) = \frac{\partial w_\delta^d(\varepsilon^0)}{\partial \varepsilon^0} \qquad \bar{\varepsilon} = \bar{\varepsilon}(\sigma^0) = \frac{\partial w_\delta^{t*}(\sigma^0)}{\partial \sigma^0}. \tag{5.4}$$

Next, we have the minimum potential energy principle

$$\Pi(\varepsilon) \le \frac{1}{2}\int_{B_\delta} w(\tilde{\varepsilon})\mathrm{d}V - \int_{\partial B'_\delta} \tilde{\mathbf{t}}\cdot\tilde{\mathbf{u}}\,\mathrm{d}S, \tag{5.5}$$

and the minimum complementary energy principle

$$\Pi(\sigma) \le \frac{1}{2}\int_{B_\delta} w(\tilde{\sigma})\mathrm{d}V - \int_{\partial B''_\delta} \tilde{\mathbf{t}}\cdot\tilde{\mathbf{u}}\,\mathrm{d}S. \tag{5.6}$$

From this, the apparent constitutive responses are shown to be related by

$$w_\delta^d(\varepsilon^0, \omega) \le w_{\delta'}^d(\varepsilon^0, \omega) \qquad \forall\ \delta' = \delta/2, \tag{5.7}$$

and

$$w_{\delta}^{t*}(\varepsilon^0,\omega) \le w_{\delta'}^{t*}(\varepsilon^0,\omega) \qquad \forall\, \delta' = \delta/2. \tag{5.8}$$

By passing to the ensemble, we get a hierarchy of bounds from above [46]

$$w_{\infty}^{d} \le \cdots \le \langle w_{\delta}^{d}\rangle \le \langle w_{\delta'}^{d}\rangle \le \cdots \le \langle w_{1}^{d}\rangle \qquad \forall\, \delta' = \delta/2, \tag{5.9}$$

and from below

$$w_{\infty}^{t*} \le \cdots \le \langle w_{\delta}^{t*}\rangle \le \langle w_{\delta'}^{t*}\rangle \le \cdots \le \langle w_{1}^{t*}\rangle \qquad \forall\, \delta' = \delta/2. \tag{5.10}$$

Note: $w_{\delta}^{t*} \neq \sigma : \varepsilon^0 - w_{\delta}^{d}$ because the mesoscale response depends on the type of loading.

5.1.2. Power-law nonlinear elastic materials

Consider a random medium governed pointwise by this constitutive law [18]

$$\begin{aligned} \sigma = \sigma(\varepsilon) &= \sum_{n=1}^{N} \mathbf{C}_n : \varepsilon^n = \frac{\partial w(\varepsilon)}{\partial \varepsilon} \\ \varepsilon = \varepsilon(\sigma) &= \sum_{n=1}^{N} \mathbf{S}_n : \sigma^n = \frac{\partial w^*(\sigma)}{\partial \sigma}, \end{aligned} \tag{5.11}$$

While the above forms are of mechanical form, the energetic laws are

$$w(\varepsilon) = \sum_{n=1}^{N} \mathbf{C}_n : \frac{\varepsilon^n}{n+1} \qquad w^*(\sigma) = \sum_{n=1}^{N} \mathbf{S}_n : \frac{\sigma^n}{n+1}. \tag{5.12}$$

This leads to apparent responses as

$$\begin{aligned} \bar{\sigma} &= \sum_{n=1}^{N} C_{n\delta}^{d}(\omega) : (\varepsilon^0)^n = \frac{\partial w_{\delta}^{d}(\varepsilon^0)}{\partial \varepsilon^0} \\ \bar{\varepsilon} &= \sum_{n=1}^{N} \mathbf{S}_{n\delta}^{t}(\omega) : (\sigma^0)^n = \frac{\partial w_{\delta}^{t*}(\sigma^0)}{\partial \sigma^0}. \end{aligned} \tag{5.13}$$

and

$$w(\bar{\varepsilon}) = \sum_{n=1}^{N} \mathbf{C}_n : \frac{\bar{\varepsilon}^n}{n+1} \qquad w^*(\bar{\sigma}) = \sum_{n=1}^{N} \mathbf{S}_n : \frac{\bar{\sigma}^n}{n+1}. \tag{5.14}$$

The apparent constitutive laws for $B_{\delta}(\omega)$ are next shown to be related by a partition theorem [44,45]

$$(\mathbf{S}_{n\delta}^{t}(\omega))^{-1} \le \mathbf{C}_{n\delta}^{\mathrm{eff}}(\omega) \le \mathbf{C}_{n\delta}^{d}(\omega), \tag{5.15}$$

and, in view of the statistical homogeneity and ergodicity of the material, we have hierarchies of bounds from above

$$\mathbf{C}_{n\infty}^{d} \le \cdots \le \langle \mathbf{C}_{n\delta}^{d}\rangle \le \langle \mathbf{C}_{n\delta'}^{d}\rangle \le \cdots \le \langle \mathbf{C}_{n1}^{d}\rangle \qquad \forall\, \delta' = \delta/2, \tag{5.16}$$

and from below

$$\mathbf{S}_{n\infty}^{t} \le \cdots \le \langle \mathbf{S}_{n\delta}^{t}\rangle \le \langle \mathbf{S}_{n\delta'}^{t}\rangle \le \cdots \le \langle \mathbf{S}_{n1}^{t}\rangle \qquad \forall\, \delta' = \delta/2. \tag{5.17}$$

It is known that, under proportional monotonic loading, strain-hardening elastoplastic composites may be treated in the framework of deformation theory of plasticity, which is formally equivalent to physically nonlinear, small-deformation elasticity, such as dealt with here. In [46] we assumed this equivalence to also hold for apparent elastoplastic response, and have thus obtained energy bounds on random elastoplastic composites. In that reference we have also proposed an approach via tangent moduli. Finally, the effect of imperfect interfaces on the hierarchies of bounds has been investigated by Hazanov [45].

5.1.3. Finite elasticity

The key assumption of the finite hyperelasticity theory is the existence of a strain energy function ψ per unit volume of an undeformed body, which depends on the deformation of the object and its material properties. Here we restrict ourselves to the reference configuration, so that, the equation of state of the material takes the form:

$$P_{ik} = \frac{\partial \psi}{\partial F_{ik}}. \tag{5.18}$$

Here P_{ik} is the first Piola–Kirchhoff stress tensor and F_{ik} is the deformation gradient tensor.

In analogy to Section 2.2, consider two types of boundary conditions: uniform displacement gradient F_{ik}^0 is prescribed:

$$u_i(\mathbf{x}) = (F_{ik}^0 - \delta_{ik}^0)x_i \qquad \forall\, \mathbf{x} \in \partial B_{\delta}, \tag{5.19}$$

or uniform traction where P_{ik}^0 is prescribed:

$$t_i(\mathbf{x}) = P_{ik}^0 n_k \qquad \forall\, \mathbf{x} \in \partial B_{\delta}. \tag{5.20}$$

Next, we consider the functional

$$\Pi(\tilde{\mathbf{u}}) = \int_{B_{\delta}} \psi(\tilde{u}_{i,k}) dV - \int_{\partial B_{\delta}^{t}} t_i^0 \tilde{u}_i \mathrm{d}S, \tag{5.21}$$

where $\tilde{\mathbf{u}}$ is an admissible displacement field such that $\tilde{\mathbf{u}} = \mathbf{u}$ on the portion of the boundary ∂B_{δ}^{u} where displacement is prescribed, and t_i^0 is the specified boundary traction on the remaining part of $(B_{\delta}$. This is the counterpart of the principle of minimum potential energy for infinitesimal elastic deformation in finite elasticity in that the functional $\Pi(\tilde{\mathbf{u}})$ assumes a local minimum for the actual solution $\mathbf{u}$ if

$$\int_{B_{\delta}} \frac{\partial^2 \psi}{\partial u_{i,k} \partial u_{p,q}} d_{i,k} d_{p,q} \mathrm{d}V = 0, \tag{5.22}$$

for all non-zero d_i such that $d_i = 0$ on ∂B_{δ}^{u} [46].

By proceeding in a fashion analogous to Section 4.1, we get a hierarchy of bounds on the energy density of the RVE $(\Psi_{\infty}(\mathbf{F}^0))$ from above

$$\begin{aligned} &\Psi_{\infty}(\mathbf{F}^0) \le \cdots \le \langle \Psi_{\delta}(\mathbf{F}^0)\rangle \le \langle \Psi_{\delta'}(\mathbf{F}^0)\rangle \le \cdots \le \langle \Psi_{1}(\mathbf{F}^0)\rangle \\ &\forall \delta' = \delta/2, \end{aligned} \tag{5.23}$$

We now turn to the derivation of a reciprocal expression for the lower bounds. Since in nonlinear elasticity, the strain-energy function can be non-convex and therefore non-invertible, we employ the functional first proposed by Lee

and Shield [47]

$$Q(\tilde{\mathbf{u}}) = \int_{B_\delta} \left(\frac{\partial \psi}{\partial \tilde{u}_{ik}} \tilde{u}_{ik} - \psi \right) dV - \int_{\partial B'_\delta} \frac{\partial \psi}{\partial \tilde{u}_{ik}} n_k \tilde{u}_i dS. \tag{5.24}$$

Here $\tilde{u}_{ik}$ is a trial function, which satisfies the following conditions:

$$\frac{\partial}{\partial x_k}\left(\frac{\partial \psi}{\partial \tilde{u}_{i,k}} \right) = 0 \text{ in } B_\delta, \qquad \frac{\partial \psi}{\partial \tilde{u}_{i,k}} n_k = t_i^0 \text{ on } \partial B'_\delta. \tag{5.25}$$

It was shown that the functional Q is stationary for $\tilde{u}_{ik} = u_{ik}$, where u_i, the actual solution of a problem, assumes a local minimum if

$$\int_{B_\delta} \frac{\partial^2 \psi}{\partial u_{i,k} \partial u_{p,q}} d_{ik} d_{pq} \mathrm{d}V > 0$$

for all nonzero d_{ik} satisfying the following conditions:

$$\begin{aligned} &\frac{\partial}{\partial x_k}\left(\frac{\partial^2 \psi}{\partial u_{i,k} \partial u_{p,q}} d_{pq} \right) = 0 \text{ in } B_\delta, \\ &\frac{\partial^2 \psi}{\partial u_{i,k} \partial u_{p,q}} d_{pq} n_k = 0 \text{ on } \partial B'_\delta. \end{aligned} \tag{5.26}$$

Again, by following the path employed for linear elastic random media, we can derive a scale dependent hierarchy of lower bounds on the effective property $Q_\infty(\mathbf{F}^0)$

$$\begin{aligned} &Q_\infty(\mathbf{F}^0) \le \cdots \le \langle Q_\delta(\mathbf{F}^0) \rangle \le \langle Q_{\delta'}(\mathbf{F}^0) \rangle \le \cdots \le \langle Q_1(\mathbf{F}^0) \rangle \\ &\forall \delta' = \delta/2. \end{aligned} \tag{5.27}$$

Now, noting that $\partial\psi/\partial\tilde{u}_{ik} \quad \tilde{u}_{ik}$ can be equivalently expressed as $\mathbf{P}$: $\mathbf{F}$, (5.24) becomes

$$Q(\tilde{u}_{ik}, \omega) = \overline{\mathbf{P} : \mathbf{F}} - \psi(\mathbf{P}^0, \omega) = \mathbf{P}^0 : \bar{\mathbf{F}} - \psi(\mathbf{P}^0, \omega), \tag{5.28}$$

where the bar denotes a volume average, and averaging theorems [48,70] have been employed. Ultimately, (5.23) and (5.27) can be combined to result in a hierarchy of mesoscale bounds on the effective energy function of a composite material at finite strains [49,50]:

$$\begin{aligned} &-\langle Q_1(\mathbf{P}^0) \rangle \le \cdots \le -\langle Q_{\delta'}(\mathbf{P}^0) \rangle \le -\langle Q_\delta(\mathbf{P}^0) \rangle \le \cdots \le Q_\infty(\mathbf{P}^0) \\ &= \Psi_\infty(\mathbf{F}^0) \le \cdots \le \langle \Psi_\delta(\mathbf{F}^0) \rangle \le \langle \Psi_{\delta'}(\mathbf{F}^0) \rangle \le \cdots \le \langle \Psi_1(\mathbf{F}^0) \rangle \\ &\times \forall \delta' = \delta/2. \end{aligned} \tag{5.29}$$

5.2. Elastic–plastic materials

Let us now consider a multiphase ($p = 1, \ldots, p_{\text{tot}}$) elastic-plastic-hardening material described by an associated flow rule (e.g. [28])

$$\begin{aligned} \mathrm{d}\varepsilon'_{ij} &= \frac{d\sigma'_{ij}}{2G_p} + \lambda \frac{\partial f}{\partial \sigma_{ij}} \mathrm{d}f_p \quad \text{whenever} \quad f_p = c_p \text{and} \mathrm{d}f \ge 0 \\ \mathrm{d}\varepsilon'_{ij} &= \frac{d\sigma'_{ij}}{2G_p} \qquad\qquad\quad \text{whenever} \quad f_p < c_p \\ \mathrm{d}\varepsilon &= \frac{1 - 2\nu_p}{2G_p(1+\nu_p)} \mathrm{d}\sigma \qquad \text{everywhere} \quad (\mathrm{d}\varepsilon = \mathrm{d}\varepsilon_{ii}/3 \mathrm{d}\sigma = \mathrm{d}\sigma_{ii}/3) \end{aligned} \tag{5.30}$$

where G_p (shear modulus), ν_p (Poisson's ratio), and c_p (yield limit) form a vector, whose each component (described by its indicator function χ_p) gives rise to a scalar random field, such as

$$G(\omega, \mathbf{x}) = \sum_{p=1}^{p_{\text{tot}}} G_p \chi_p(\omega, \mathbf{x}) \, \forall \, \omega \in \Omega. \tag{5.31}$$

The entire body $\mathcal{B} = \{B(\omega); \omega \in \Omega\}$ is described by a random vector field $\Theta = \{G, \nu, c\}$.

First, note that the results of Section 5.1.1 can be applied to the loading, although not the unloading, response regime. Next, we can consider tangent moduli. Thus, on the mesoscale we have tangent moduli—$\mathbf{C}^{\mathrm{T}}_\delta(\omega)$ or $\mathbf{S}^{\mathrm{T}}_\delta(\omega)$—of the body $B_\delta(\omega)$, which connect stress increments with strain increments applied to it

$$\mathrm{d}\sigma = \mathbf{C}^{\mathrm{T}}_\delta(\omega) : \mathrm{d}\varepsilon \quad \mathrm{d}\varepsilon = \mathbf{S}^{\mathrm{T}}_\delta(\omega) : \mathrm{d}\sigma. \tag{5.32}$$

Consequently, the Hill condition, and its implication for the type of admissible boundary conditions, is

$$\overline{\mathrm{d}\sigma : \mathrm{d}\varepsilon} = \mathrm{d}\bar{\sigma} : \overline{\mathrm{d}\varepsilon} \Leftrightarrow \int_{\partial B_\delta} (\mathrm{d}\,\mathbf{t} - \mathrm{d}\bar{\sigma} \cdot \mathbf{n}) \cdot (\mathrm{d}\,\mathbf{u} - \mathrm{d}\,\bar{\varepsilon} \cdot \mathbf{x}) \mathrm{d}S = 0, \tag{5.33}$$

where $\mathrm{d}\bar{\sigma} = \mathrm{d}\sigma^0$ and $\mathrm{d}\bar{\varepsilon} = \mathrm{d}\varepsilon^0$. Thus, $\mathbf{u}$ and ε should be replaced by $\mathrm{d}\mathbf{u}$ and $\mathrm{d}\varepsilon$ in both (2.11) and (2.13).

Next, we recall two extremum principles (e.g. [28]): one for kinematically admissible fields

$$\int_{\partial B'_\delta} \mathrm{d}\mathbf{t} \cdot \mathrm{d}\tilde{\mathbf{u}} \, \mathrm{d}S - \frac{1}{2} \int_{B_\delta} \mathrm{d}\tilde{\sigma} : \mathrm{d}\tilde{\varepsilon} \mathrm{d}V \le \int_{\partial B'_\delta} \mathrm{d}\mathbf{t} \cdot \mathrm{d}\mathbf{u} \, \mathrm{d}S - \frac{1}{2} \int_{B_\delta} \mathrm{d}\sigma : \mathrm{d}\varepsilon \mathrm{d}V, \tag{5.34}$$

and another for statically admissible fields

$$\frac{1}{2} \int_{B_\delta} \mathrm{d}\sigma \cdot \mathrm{d}\varepsilon \, \mathrm{d}V - \int_{\partial B''_\delta} \mathrm{d}\mathbf{t} \cdot \mathrm{d}\mathbf{u} \, \mathrm{d}S \le \frac{1}{2} \int_{B_\delta} \mathrm{d}\tilde{\sigma} : \mathrm{d}\tilde{\varepsilon} \, \mathrm{d}V - \int_{\partial B''_\delta} \mathrm{d}\tilde{\mathbf{t}} \cdot \mathrm{d}\mathbf{u} \, \mathrm{d}S. \tag{5.35}$$

From this, we find

$$\mathbf{C}^{\mathrm{Td}}_\delta(\omega) \le \mathbf{C}^{\mathrm{Td}}_{\delta'}(\omega), \quad \mathbf{S}^{\mathrm{Tt}}_\delta(\omega) \le \mathbf{S}^{\mathrm{Tt}}_{\delta'}(\omega), \quad \forall \delta' = \delta/2. \tag{5.36}$$

Upon ensemble averaging, and applying this to ever larger windows *ad infinitum* we get a hierarchy of bounds on

the macroscopically effective tangent modulus $\mathbf{C}_\infty^{\mathrm{T}} = \left(\mathbf{S}_\infty^{\mathrm{T}}\right)^{-1}$

$$\langle \mathbf{S}_1^{\mathrm{Tt}} \rangle^{-1} \leq \cdots \leq \langle \mathbf{S}_{\delta'}^{\mathrm{Tt}} \rangle^{-1} \leq \langle \mathbf{S}_{\delta}^{\mathrm{Tt}} \rangle^{-1} \leq \cdots \leq \mathbf{C}_\infty^{\mathrm{T}} \leq \cdots \leq \langle \mathbf{C}_{\delta}^{\mathrm{Td}} \rangle$$

$$\leq \langle \mathbf{C}_{\delta'}^{\mathrm{Td}} \rangle \leq \cdots \leq \langle \mathbf{C}_1^{\mathrm{Td}} \rangle, \quad \forall \delta' = \delta/2 \tag{5.37}$$

where $\langle \mathbf{S}_1^{\mathrm{Tt}} \rangle^{-1}$ and $\langle \mathbf{C}_1^{\mathrm{Td}} \rangle$ are recognized as the Sachs and Taylor bounds, respectively. See [71] for a comprehensive reviews of effective (RVE level) properties of nonlinear composites.

Indeed, one particular problem we studied involved a matrix-inclusion composite material [46], with the matrix phase being elastic–hardening plastic, and the inclusions being elastic and, indeed, of the same modulus as that of the matrix in the elastic range, see also the recent review [51]. Here we display the bounding character of responses computed under (2.11) and (2.12), respectively, for elastic–plastic materials with both phases being elastic-hardening plastic [52,53]. Patterns of plastic shear bands under these two boundary conditions are displayed in Fig. 11, while the corresponding hierarchy of bounds, computed here on two scales, is shown in Fig. 12. Note:

(i) at a smaller scale ($\delta = 6$), the response under uniform kinematic (2.11) is much more uniform than that under uniform stress boundary conditions (2.12);
(ii) at a larger scale ($\delta = 15$), the discrepancy due to different types of loading is much smaller, which shows a tendency to homogenize with δ tending to ∞;
(iii) the macroscopic response is better (in fact, quite well) approximated by the uniform stress than by the uniform strain assumption. This situation would be reversed for an elastic–plastic matrix with soft, rather than hard, inclusions, and helps explain why Taylor bound works well for polycrystals with dislocations.

Another setting where mesoscale tangent moduli of power-law hardening materials have recently been employed is the mechanics of paper [54].

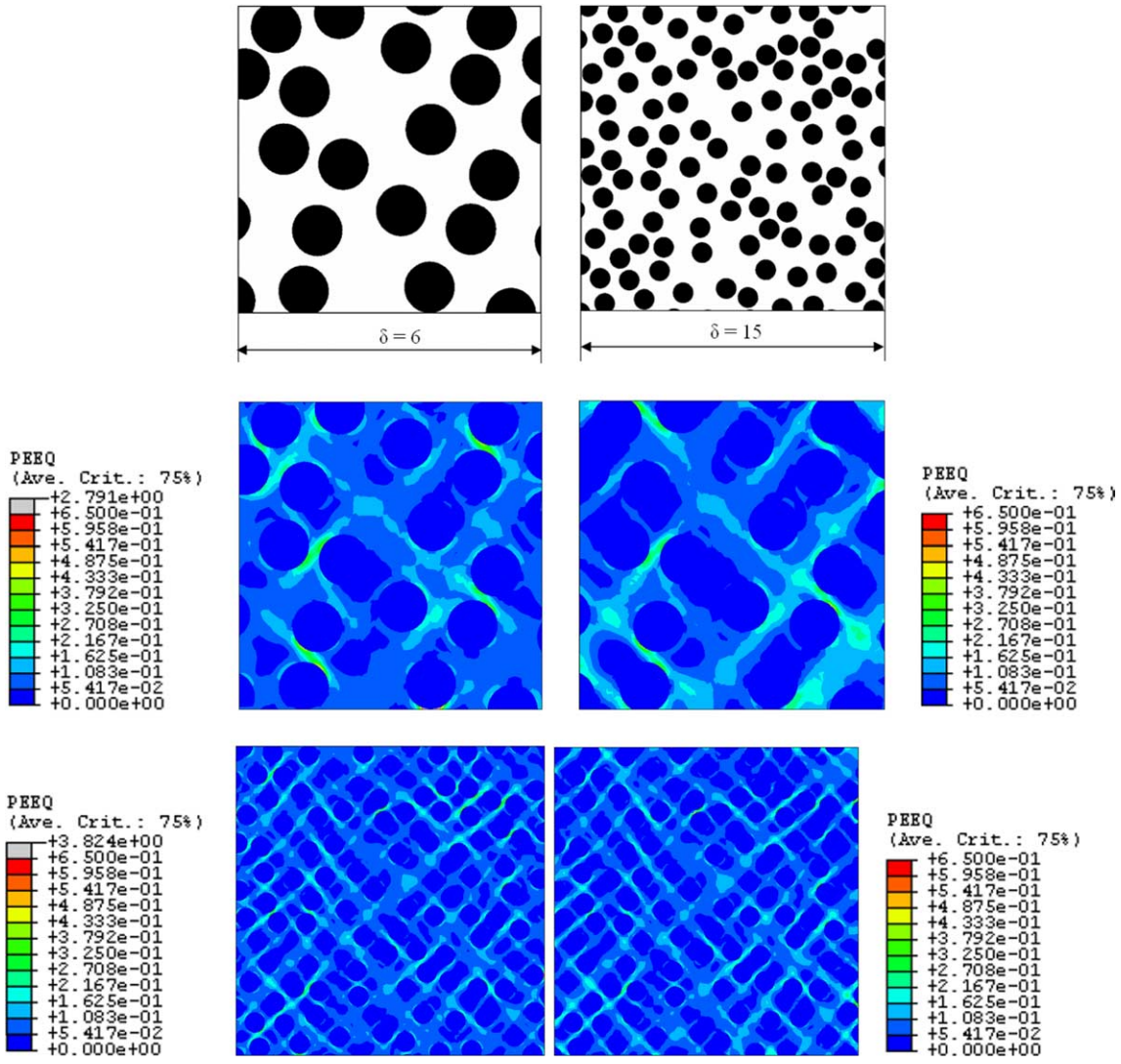

Fig. 11. (a) Two realizations of a random matrix-inclusion composite at mesoscales $\delta = 6$ and $\delta = 15$. (b) and (c) Contour plots of equivalent plastic strain of the matrix-inclusion composite of Figs. (a, b) under displacement (left) and traction (right) boundary conditions at $\delta = 6$ and 15, respectively; after [53].

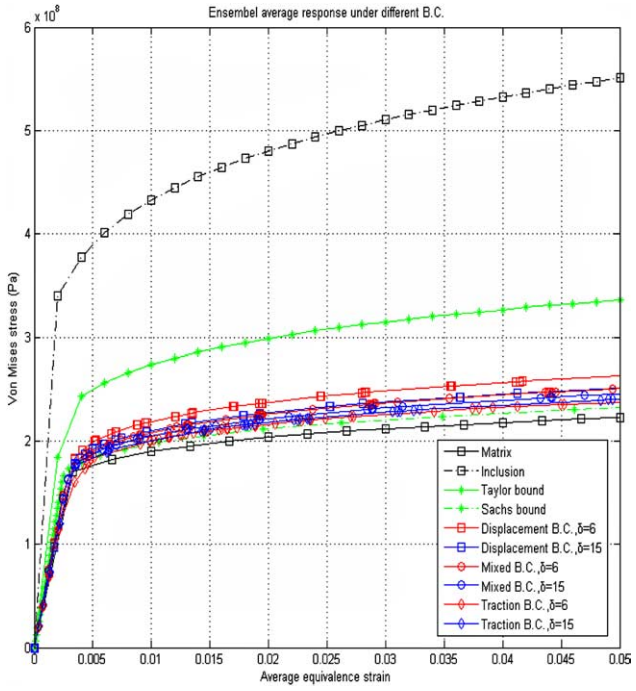

Fig. 12. Ensemble average stress-strain responses of matrix-inclusion composites for different mesoscales δ, under different boundary conditions [53].

5.3. Rigid-perfectly plastic materials

Here a random rigid–plastic material $\mathcal{B}=\{B(\omega);\omega\in\Omega\}$, $\forall\omega\in\Omega$, is defined by stating that, for any grain (i.e. on microscale),

$$d_{ij}=\lambda\frac{\partial F(\sigma_{ij},\omega)}{\partial\sigma_{ij}},\qquad \sigma_{ij}d_{ij}=\sigma_{ij}\lambda\frac{\partial F(\sigma_{ij},\omega)}{\partial\sigma_{ij}}\geq 0. \tag{5.38}$$

Thus, in each grain the admissible stress states lie within the set

$$P_1(\omega)=\{\sigma|F(\sigma,\omega)\leq 0\}\equiv\{\sigma|\sigma_{eq}\leq\sigma_Y\}, \tag{5.39}$$

where σ_{eq} is the equivalent stress; σ_{Y} is the yield stress.

For the RVE ($\delta\to\infty$), the yield (or extremal) surface of the composite B_∞ delimits the set

$$\begin{aligned}P^{\mathrm{hom}}=\{&\Sigma\in\mathbb{R}^{3\times3}|\,\exists\,\sigma(\mathbf{x})\text{ with }\bar{\sigma}=\Sigma,\\ &div\sigma=0,\ F(\sigma,\omega)\leq 0,\ \forall\,\mathbf{x}\in B\},\end{aligned} \tag{5.40}$$

and the elementary Taylor and Sachs bounds on P^{hom} are expressed via a hierarchy of inclusion relations

$$\left\{\sum|\sum_{eq}\leq\inf_{\mathbf{x}\in B_\delta}\sigma_Y(\mathbf{x})\right\}^{\mathrm{Sachs}}\subset P^{\mathrm{hom}}$$

$$\subset\left\{\sum|\sum_{eq}\leq\overline{\sigma_Y}\right\}^{\mathrm{Taylor}}. \tag{5.41}$$

On any finite mesoscale—a scale below RVE—there holds some form of an apparent yield surface $F_\delta(\bar{\sigma},\omega)$, bounding some set

$$P_\delta(\omega)=\{\bar{\sigma}_\delta|\,\exists\,\sigma(\mathbf{x}),\quad div\sigma=0,\ F(\sigma,\omega)\leq 0,\quad\forall\mathbf{x}\in B_\delta\}. \tag{5.42}$$

In contradistinction to P^{hom}, $P_\delta(\omega)$ depends on the configuration ω and the mesoscale δ.

The starting point is provided by the upper bound theorem allowing for discontinuities in the velocity field [55]

$$\int_{\partial B_\delta}\mathbf{t}\cdot\tilde{\mathbf{v}}\,\mathrm{d}S=\int_{B_\delta}\tilde{\sigma}:\tilde{\mathbf{d}}\,\mathrm{d}V+\int_{S^{[v^*]}}\tau_Y|[\tilde{\mathbf{v}}]|\mathrm{d}S, \tag{5.43}$$

where $\tilde{\mathbf{v}}$ is an arbitrary kinematically admissible velocity field, $\tilde{\sigma}$ an associated stress field, and $S^{[v^*]}=\cup_{m=1}^{M}S_m^{[v^*]}$ is the set of internal surfaces of discontinuity in v^*. With this Ansatz, we showed in [51] that

$$\hat{P^v_\delta}\subseteq\hat{P^v_{\delta'}}\quad\forall\,\delta'<\delta, \tag{5.44}$$

where $\hat{P^v_\delta}$ and $\hat{P^v_{\delta'}}$ denote two domains in stress space bounded, respectively, by the ensemble average yield surfaces $\langle F^v_\delta\rangle$ and $\langle F^v_{\delta'}\rangle$. By induction, this leads to a hierarchy of inclusions

$$P^v_\infty\subseteq\ldots\subseteq\hat{P^v_\delta}\subseteq\hat{P^v_{\delta'}}\subseteq\ldots\subseteq\hat{P^v_1}\quad\forall\,\delta'=\delta/2, \tag{5.45}$$

where P^v_∞ is the yield locus P^{hom} of RVE. On the other hand, $\hat{P^v_1}$ is the domain bounded by the average yield locus of a single grain, or the Taylor bound of (5.29), which results from prescribing a uniform deformation rate field everywhere.

While an analytical derivation of a lower hierarchy of bounds under uniform traction boundary conditions is not available, our computational results lead us to conjecture that this hierarchy of inclusions holds

$$P^t_\infty\supseteq\ldots\supseteq\hat{P^t_\delta}\supseteq\hat{P^t_\delta}\supseteq\ldots\supseteq\hat{P^t_1}\qquad\forall\,\delta'=\delta/2. \tag{5.46}$$

Here $\hat{P^t_\delta}$ and $\hat{P^t_{\delta'}}$ denote domains in stress space bounded by ensemble averaged yield surfaces $\langle F^t_\delta\rangle$ and $\langle F^t_{\delta'}\rangle$. More information is given in the recent review [51].

5.4. Viscoelastic materials

Here we give a brief account of research carried out by Huet [2,56,57], First, the Hill condition now involves strain rates

$$\overline{\sigma:\dot{\varepsilon}}=\bar{\sigma}:\dot{\bar{\varepsilon}}. \tag{5.47}$$

Translated to the mesoscale, it implies that

$$\overline{\sigma:\dot{\varepsilon}}=\bar{\sigma}:\dot{\varepsilon}^0\quad\text{or}\quad\sigma^0:\dot{\bar{\varepsilon}}, \tag{5.48}$$

depending on whether the strain rate ($\dot{\varepsilon}^0$) or stress ($\boldsymbol{\sigma}^0$) is prescribed.

On the microscale (i.e. locally) the material is governed by a formula involving a relaxation modulus tensor ($\mathbf{r}$)

$$\sigma(t)=\int_0^t\mathbf{r}(t-t'):d\varepsilon(t')\mathrm{d}t, \tag{5.49}$$

or a dual one involving a creep compliance tensor (**f**)

$$\varepsilon(t) = \int_0^t \mathbf{f}(t-t') : \mathrm{d}\sigma(t')\mathrm{d}t. \tag{5.50}$$

On the mesoscale, under the kinematic boundary condition, the material domain $B(\omega)$ is governed by a formula involving a relaxation modulus tensor ($\mathbf{r}_\delta$)

$$\bar{\sigma}(t) = \int_0^t \mathbf{r}_\delta(t-t') : \mathrm{d}\varepsilon^0(\mathbf{x}, t')\mathrm{d}t, \tag{5.51}$$

and, under the traction boundary condition, a similar one involving a creep compliance tensor ($\mathbf{f}_\delta$)

$$\bar{\varepsilon}(t) = \int_0^t \mathbf{f}_\delta(t-t') : \mathrm{d}\sigma^0(\mathbf{x}, t')\mathrm{d}t. \tag{5.52}$$

On the macroscale the two tensors become dual, and then we have $\mathbf{r}^{\mathrm{eff}}(t)$ and $\mathbf{f}^{\mathrm{eff}}(t)$. Now, Huet has shown that $\mathbf{r}^{\mathrm{eff}}(t)$ is bounded by the hierarchy

$$\begin{aligned} &\mathbf{r}^{\mathrm{eff}}(t) \le \cdots \le \langle \mathbf{r}_\delta(t) \rangle \le \langle \mathbf{r}_\delta(t) \rangle \le \cdots \le \langle \mathbf{r}_1(t) \rangle \\ &\forall \delta' = \delta/2, \ \ \forall\, t \ge 0, \end{aligned} \tag{5.53}$$

and $\mathbf{f}^{\mathrm{eff}}(t)$ is bounded by the hierarchy

$$\begin{aligned} &\mathbf{f}^{\mathrm{eff}}(t) \le \cdots \le \langle \mathbf{f}_\delta(t) \rangle \le \langle \mathbf{f}_\delta(t) \rangle \le \cdots \le \langle \mathbf{f}_1(t) \rangle \\ &\forall \delta' = \delta/2, \ \ \forall\, t \ge 0. \end{aligned} \tag{5.54}$$

A number of related results on that subject are in the papers referenced above.

5.5. Thermoelastic materials

Let us now consider a linear thermoelastic composite material, e.g. [58,59]. Each specimen $B(\omega) \in \mathcal{B}$ is now described locally by

$$\begin{aligned} &\varepsilon_{ij} = S_{ijkl}(\omega, \mathbf{x})\sigma_{kl} + \alpha_{ij}(\omega, \mathbf{x})\Delta T \quad \text{or} \\ &\sigma_{ij} = C_{ijkl}(\omega, \mathbf{x})\varepsilon_{kl} + \Gamma_{ij}(\omega, \mathbf{x})\Delta T, \end{aligned} \tag{5.55}$$

where $S_{ijkl}(\omega, \mathbf{x}) = C^{-1}_{ijkl}(\omega, \mathbf{x})$, ΔT is a temperature rise, and

$$\Gamma_{ij}(\omega, \mathbf{x}) = -C_{ijkl}(\omega, \mathbf{x})\alpha_{kl}(\omega, \mathbf{x}) \tag{5.56}$$

are the thermal stress coefficients computed from the thermal expansion coefficients α_{kl}. Of interest is the derivation of scale dependent bounds on $\boldsymbol{\alpha}^{\mathrm{eff}} \equiv \boldsymbol{\alpha}_\infty$ using the already available bounds on $\mathbf{C}^{\mathrm{eff}} \equiv \mathbf{C}_\infty$. Note here that

$$\Gamma^{\mathrm{eff}}_{ij}(\omega, \mathbf{x}) = -C^{\mathrm{eff}}_{ijkl}(\omega, \mathbf{x})\alpha^{\mathrm{eff}}_{kl}(\omega, \mathbf{x}). \tag{5.57}$$

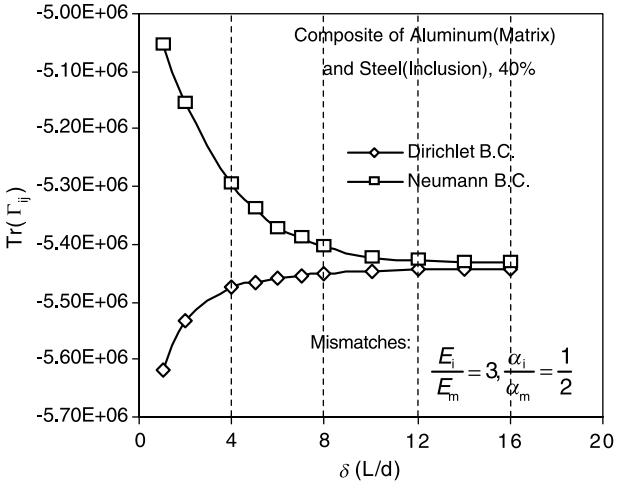

Fig. 13. Effect of increasing window scale on the hierarchies (5.64) and (5.65) of lower and upper bounds on the macroscopic thermal expansion (strain) coefficient [61].

As shown in the works referenced above, the (macroscopically) effective thermal expansion coefficients $\alpha^{\mathrm{eff}}(=\alpha^{\mathrm{eff}}_{kl})$ can be derived in terms of the effective moduli $\mathbf{C}^{\mathrm{eff}}(=C^{\mathrm{eff}}_{ijkl} = (S^{\mathrm{eff}}_{ijkl})^{-1})$ and the information on distribution of individual phases. That is, in the case of two phases 1 and 2,

$$\alpha^{\mathrm{eff}}_{ij} = (\alpha^{(1)}_{kl} - \alpha^{(2)}_{kl})P_{klmn}(S^{\mathrm{eff}}_{mnij} - S^{(2)}_{mnij}) + \alpha^{(2)}_{ij}, \tag{5.58}$$

where

$$P_{klmn}(S^{\mathrm{eff}}_{mnrs} - \bar{S}_{mnrs}) = I_{klrs} = \frac{1}{2}(\delta_{kr}\delta_{ls} + \delta_{ks}\delta_{lr}). \tag{5.59}$$

Alternatively, as pointed out in the aforementioned works, bounds on $\boldsymbol{\alpha}^{\mathrm{eff}}$ can be obtained using bounds on $\mathbf{C}^{\mathrm{eff}}$, and such a result was produced employing the Hashin–Shtrikman bounds. Of course, these derivations provide no information on the SVE and its trend to RVE. In a current study [60,61], by taking advantage of (4.12) and using the minimum energy principles of thermoelasticity, the following hierarchies of bounds have been derived for stationary and ergodic random media:

on $\boldsymbol{\alpha}_\infty$ from above

$$\alpha_\infty \le \cdots \le \langle \alpha^t_\delta \rangle \le \langle \alpha^t_{\delta'} \rangle \le \cdots \le \langle \alpha^t_1 \rangle \qquad \forall\, \delta' = \delta/2, \tag{5.60}$$

and on Γ_∞ from above

$$\Gamma_\infty \le \cdots \le \langle \Gamma^d_\delta \rangle \le \langle \Gamma^d_{\delta'} \rangle \le \cdots \le \langle \Gamma^d_1 \rangle \qquad \forall\, \delta' = \delta/2. \tag{5.61}$$

In view of (5.49), this provides a two-sided bounding hierarchy on $\boldsymbol{\alpha}_\infty$, or, equivalently, on $\boldsymbol{\Gamma}_\infty$.

These hierarchies have been computed for a planar two-phase composite material with circular shaped inclusions, at 40% volume fraction of inclusions, recall, e.g. Fig. 1. [Here a finite element mesh, again much finer than the single

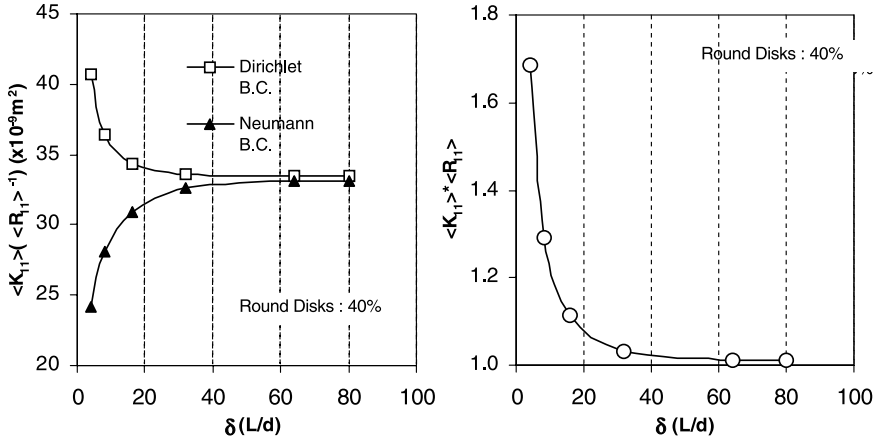

Fig. 14. (a) Effect of increasing window scale on the convergence of the permeability/resistance tensor hierarchy. (b) Scale effect on the convergence of $\mathbf{R}^n_{11}\mathbf{K}^e_{11}$ [59].

inclusion, was employed.] Taking the aluminum for the matrix and steel for the inclusions, the contrast in moduli is $E^{(i)}/E^{(m)}=1/3$, while the contrast in thermal expansion coefficients is $\alpha^{(i)}/\alpha^{(m)}=0.5$. The scale dependencies of Tr $(\mathbf{\Gamma}_\delta)$ and Tr $(\boldsymbol{\alpha}_\delta)$, following from the Neumann and Dirichlet boundary value problems, are displayed in Fig. 13. Clearly, this property asymptotes with δ increasing, and the RVE is attained at and beyond, say, $\delta=10$.

Du [60] also gives computed physical examples of (5.52, 5.53) and obtains related hierarchies on the specific heat coefficient.

5.6. Permeable materials

In phenomenological, deterministic continuum mechanics, fluid flow in porous media is described by Darcy's law. With the slow flow in a porous medium also considered as incompressible and viscous, Darcy's law is governed by the equations [62]:

$$\mathbf{U}_D=-\frac{\mathbf{K}}{\mu}\cdot\nabla p \qquad \nabla\cdot\mathbf{U}_D=g(\mathbf{x}), \tag{5.62}$$

where $\mathbf{U}_D$ is the average (or Darcy) velocity, $\bigtriangledown p$ is the applied pressure gradient driving the flow, μ is the fluid viscosity, and $\mathbf{K}$ is the permeability, a second-rank tensor which depends on the microstructure of the porous medium. Eq. $(5.62)_2$ is the continuity equation with $g(\mathbf{x})$ being the source/sink term. By defining the resistance tensor $\mathbf{R}=\mathbf{K}^{-1}$ for porous media, we can rewrite Darcy's law as

$$\nabla p=-\mu\mathbf{R}\cdot U_D. \tag{5.63}$$

We now recall the variational principle stating that, among the admissible solutions of flow field in porous media, the actual solution has a minimum value of dissipation rate [63,64]. Note here that the potential and complementary 'dissipation energy' (ϕ^p and ϕ^c) representations are, respectively,

$$\phi^p=\nabla p\frac{\mathbf{K}}{\mu}\nabla p \qquad \phi^c=\mathbf{U}_D\cdot\mu\mathbf{R}\cdot\mathbf{U}_D \tag{5.64}$$

Next, with $\bigtriangledown p^0$ being a constant pressure gradient, and $\mathbf{U}^0_D$ being a constant velocity, consider either essential (^{e}) or natural (^{n}) uniform boundary conditions [59]:

$$\begin{aligned} &p(\mathbf{x})=\nabla p^0\cdot\mathbf{x} \qquad \forall\,\mathbf{x}\in\partial B_\delta,\\ &\mathbf{U}_D(\mathbf{x})\cdot n=\mathbf{U}^0_D\cdot n \qquad \forall\,\mathbf{x}\in\partial B_\delta. \end{aligned} \tag{5.65}$$

In the first case we find $\mathbf{K}^e_\delta$, and in the second case $\mathbf{R}^n_\delta$. Employing the variational principles, and proceeding in the same fashion as for other types of materials, a hierarchy of mesoscale bounds on the effective permeability $\mathbf{K}^{eff}_\delta=(\mathbf{R}^{eff}_\delta)^{-1}$ of porous media is obtained as follows

$$\begin{aligned} &\langle\mathbf{R}^e_1\rangle^{-1}\le\cdots\le\langle\mathbf{R}^e_{\delta'}\rangle^{-1}\le\langle\mathbf{R}^e_\delta\rangle^{-1}\le\cdots\le(\mathbf{R}^{\mathrm{eff}})^{-1}\\ &\quad=\mathbf{K}^{\mathrm{eff}}\le\cdots\le\langle\mathbf{K}^n_\delta\rangle\le\langle\mathbf{K}^n_{\delta'}\rangle\le\cdots\le\langle\mathbf{K}^n_1\rangle \end{aligned} \tag{5.66}$$

$$\forall\delta'=\delta/2.$$

Fig. 14(a) illustrates this hierarchy for a 2D flow in a bed of circular disks randomly distributed by a planar Poisson point process, at porosity 0.6. This figure clearly shows the convergent trend of the upper and lower bounds in (5.66) towards macroscopically effective permeability of the porous medium. Clearly, the RVE is attained with a high accuracy on the length scales some 80 times larger than the disk size. Overall, the ongoing studies [60] indicate that the higher is the density of random disks—or, equivalently, the narrower are the micro-channels in the system—the smaller is the size of RVE for Darcy flow. Consequently, the left-side inequality in (1.1) may then be simply taken as $<$.

According to $\mathbf{K}^{\mathrm{eff}}_\delta=(\mathbf{R}^{\mathrm{eff}}_\delta)^{-1}$, we can expect an identity tensor from the product of $\mathbf{R}^n_\delta\cdot\mathbf{K}^e_\delta$ at the RVE level. Fig. 14(b) shows this convergence towards 1 in function of mesoscale δ.

Physical subject	$u(=u_3)$	$\varepsilon(=\varepsilon_{3i})$	$\mathbf{C}(=C_{3i3j})$	$\boldsymbol{\sigma}(=\sigma_{3i})$
Anti-plane elasticity	displacement	strain	elastic moduli	stress
Thermal conductivity	temperature	thermal gradient	thermal conductivity	heat flux
Torsion	stress function	strain	shear moduli	stress
Electrical conduction	potential	intensity	electrical conductivity	current density
Electrostatics	potential	intensity	permittivity	electric induction
Magnetostatics	potential	intensity	magnetic permeability	magnetic induction
Diffusion	concentration	gradient	diffusivity	flux

6. Closure

As noted at the beginning, the material spatial randomness forces one to re-examine various basic concepts of continuum solid mechanics. In this paper we have focused on the Representative Volume Element (RVE) commonly taken for granted in most of deterministic as well as in stochastic solid mechanics, although in the latter case it is more appropriately called the Statistical Volume Element (SVE). The key issue is the scale over which homogenization is being carried out—it is called the mesoscale, separating the microscale (level of microheterogeneities) from the macroscale. As the mesoscale grows, the SVE tends to become the Representative Volume Element (RVE). This occurs in terms of two hierarchies of bounds stemming from Dirichlet and Neumann boundary value problems on the mesoscale, respectively. Unless there is some periodicity in the random medium—and this is practically never the case—the RVE is not attained exactly. The approximate attainment of the RVE—i.e. the scaling trend toward it—has to be quantified for any specific random material with the help of computational mechanics.

We review results on this subject in the settings of linear and nonlinear elasticity, plasticity, viscoelasticity, thermoelasticity, and permeability. The case of thermoelasticity demonstrates the applicability of our methodology to coupled-field problems, such as piezoelectricity or poroelasticity. Since (almost) all constitutive behaviors in continuum mechanics may be brought under the single umbrella of thermomechanics [65,66], a generalization of respective Legendre transformations of free energy and dissipation functionals to mesoscales in random media can also be pursued [67,68]. Finally, let us note that below the RVE scale one has to deal with random fields having smooth realizations, and this review provides guidance on the specification of their one-point characteristics.

Appendix A. Analogies to anti-plane elasticity

For the sake of completeness, in the table below we collect various classical analogies of problems locally governed by the Laplace equation $CT_{,\,ii}=0$ (or by $(C_{ij}T_{,\,j}=0)$ in two dimensions, where, for reference, we use the terminology of anti-plane elasticity; see also [3]

References

[1] Hill R. Elastic properties of reinforced solids: some theoretical principles. J Mech Phys Solids 1963;11:357–72.

[2] Huet C. Bounds and hierarchies for the overall properties of viscoelastic heterogeneous and composite materials. Arch Mech 1995;47(6):1125–55.

[3] Hashin Z. Analysis of composite materials—a survey. J Appl Mech 1983; 50:481.

[4] Ostoja-Starzewski M. Microstructural disorder, mesoscale finite elements, and macroscopic response. Proc Roy Soc Lond A 1999;455: 3189–99.

[5] Lemaitre J, Chaboche J-L. Mechanics of solid materials.: Cambridge University Press; 1990.

[6] Ostoja-Starzewski M. Mechanics of random materials: stochastics, scale effects, and computation. In: Jeulin D, Ostoja-Starzewski M, editors. Mechanics of random and multiscale microstructures. CISM courses and lectures. Wien: Springer-Verlag; 2001.

[7] Drugan WJ, Willis JR. A micromechanics-based nonlocal constitutive equation and estimates of representative volume element size for elastic composites. J Mech Phys Solids 1996;44:497–524.

[8] Stroeven M, Askes H, Sluys LJ. Numerical determination of representative volumes for granular materials. Comp Meth Appl Mech Eng 2004; 193:3221–38.

[9] Markov K. Elementary micromechanics of heterogeneous media. In: Markov K, Preciosi L, editors. Heterogeneous media. Basel: Birkhäuser; 2000.

[10] Kröner E. Statistical continuum mechanics CISM courses and lectures. Wien: Springer-Verlag; 1972.

[11] Kröner E. The statistical basis of polycrystal plasticity. In: Gittus J, Zarka J, Nemat-Nasser S, editors. Large deformations of solids: physical basis and mathematical modelling. Amsterdam: Elsevier; 1986.

[12] Huet C. Universal conditions for assimilation of a heterogeneous material to an effective medium. Mech Res Comm 1982;9(3):165–70.

[13] Huet C. Application of variational concepts to size effects in elastic heterogeneous bodies. J Mech Phys Solids 1990;38:813–41.

[14] Sab K. Principe de Hill et homogénéisation des matériaux aléatoires. C R Acad Sci Paris II 1991;312:1–5.

[15] Sab K. On the homogenization and the simulation of random materials. Europ J Mech, A/Solids 1992;11:585–607.

[16] Stolz C. General relationships between the micro and macro scales for the non-linear behaviour of heterogeneous media. In: Gittus J, Zarka J, editors. Modelling small deformations of polycrystals. New York: Elsevier; 1986.

[17] Hazanov S, Huet C. Order relationships for boundary conditions effect in the heterogeneous bodies smaller than the representative volume. J Mech Phys Solids 1994;42:1995–2011.

[18] Kröner E. Nonlinear elastic properties of micro-heterogeneous media. ASME J Eng Mat Tech 1994;11:325–30.

[19] Nemat-Nasser S, Hori M. Micromechanics: overall properties of heterogeneous solids. Amsterdam: North-Holland; 1993.

[20] Suquet PM, Suquet PM. Elements of homogenization for solid mechanics. In: Sanchez-Palencia E, Zaoui A, editors. Homogenization techniques for composite media, lecture notes in physics 272. Springer-Verlag; 1986. p. 193–278.

[21] Willis JR, Talbot DSR. In: Maugin GA, editor. Continuum models and discrete systems.

[22] Hazanov S, Amieur M. On overall properties of elastic heterogeneous bodies smaller than the representative volume. Int J Engng Sci 1995;23: 1289–301.

[23] Hill R. The essential structure of constitutive laws for metal composites and polycrystals. J Mech Phys Solids 1967;15:79–95.
[24] Mandel J. Plasticité classique et viscoplasticité. CISM courses and lectures. vol. 97. Wien-New York: Springer; 1972.
[25] Cristescu ND, Craciun E-M, Soós E. Mechanics of elastic composites.: Chapman & Hall/CRC Press; 2003.
[26] Terada K, Hori M, Kyoya T, Kikuchi N. Effective thermal expansion coefficients and specific heats of composite materials. Int J Solids Struct 2000;37:2285–311.
[27] Kanit T, Forest S, Galliet I, Monoury V, Jeulin D. Determination of the size of the representative volume element for random composites: statistical and numerical approach. Int J Solids Struct 2003;40: 3647–79.
[28] Hill R. The mathematical theory of plasticity. Oxford: Clarendon Press; 1950.
[29] Ostoja-Starzewski M, Wang C. Linear elasticity of planar Delaunay networks: Random field characterization of effective moduli. Acta Mech 1989;80:61–80.
[30] Huyse L, Maes MA. Random field modeling of elastic properties using homogenization. ASCE J Eng Mech 2001;127(1):27–36.
[31] Ostoja-Starzewski M. Scale effects in materials with random distributions of needles and cracks. Mech Mater 1999;31(12):883–93.
[32] Ostoja-Starzewski M. Micromechanics as a basis of random elastic continuum approximations. Probab Eng Mech 1993;8(2):107–14.
[33] Ostoja-Starzewski M. Random field models of heterogeneous materials. Intl J Solids Struct 1998;35(19):2429–55.
[34] Ostoja-Starzewski M, Schulte J. Bounding of effective thermal conductivities of multiscale materials by essential and natural boundary conditions. Phys Rev B 1996;54:278–85.
[35] Amieur M, Hazanov S, Huet C. Numerical and experimental assessment of the size and boundary conditions effects for the overall properties of granular composite bodies smaller than the representative volume. In: Parker DF, England AH, editors. IUTAM Symposium on Anisotropy, Inhomogeneity and Nonlinearity in Solid Mechanics. Kluwer Academic; 1995. p. 149–54.
[36] Cardy JL, editor. Finite-size scaling. Amsterdam: North-Holland; 1988.
[37] Ostoja-Starzewski M. Lattice models in micromechanics. Appl Mech Rev 2002;55(1):35–60.
[38] Vakulenko AA, Kachanov ML. Continuum model of medium with cracks (in Russian). Mech Solids 1971;4:54–9.
[39] Budiansky B, O'Connell RJ. Elastic moduli of a cracked solid. Int J Solids Struct 1976;12:81–97.
[40] Kachanov M. Elastic solids with many cracks and related problems. Advances in Applied Mechanics. vol. 30.: Academic Press; 1993 p. 259.
[41] Jiang M, Alzebdeh K, Jasiuk I, Ostoja-Starzewski M. Scale and boundary conditions effects in elastic properties of random composites. Acta Mech 2001;148(1–4):63–78.
[42] Garboczi EJ, Thorpe MF, DeVries MS, Day AR. Universal conductance curve for a plane containing random holes. Phys Rev A 1991;43:6473–80.
[43] Ostoja-Starzewski M. Universal material property in conductivity of planar random microstructures. Phys Rev B 2000;62(5):2980–3.
[44] Hazanov S. Hill condition and overall properties of composites. Arch Appl Mech 1998;68:385–94.
[45] Hazanov S. On apparent properties of nonlinear heterogeneous bodies smaller than the representative volume. Acta Mech 1999;138:123–34.
[46] Jiang M, Ostoja-Starzewski M, Jasiuk I. Scale-dependent bounds on effective elastoplastic response of random composites. J Mech Phys Solids 2001;49(3):655–73.
[47] Lee SJ, Shield RT. Variational principles in finite elastostatics. ZAMP 1980;31:437–53.
[48] Costanzo F, Gray GL, Andia PC. On the notion of average mechanical properties in MD simulation via homogenization. Modell Simul Mater Sci Eng 2004;12: S333–S345.
[49] Khisaeva Z. PhD Thesis (in progress). Montreal, Canada: McGill University; 2005.
[50] Khisaeva Z, Ostoja-Starzewski M. Mesoscale bounds in finite elasticity of random composites Proceedings of 20th CANCAM. Montreal, Canada: McGill University; 2005 pp. 454–455.
[51] Ostoja-Starzewski M. Scale effects in plasticity of random media: status and challenges. Int J Plast 2005;21:1119–60.
[52] Li W. PhD Thesis (in progress). Montreal, Canada: McGill University; 2005.
[53] Li W, Ostoja-Starzewski M. Elastoplasticity of random heterogeneous materials 20th Canadian Congress on Applied Mechanics—CANCAM, 465–466, Montreal, Canada 2005.
[54] Ostoja-Starzewski M, Castro J. Random formation, inelastic response, and scale effects in paper. Phil Trans Roy Soc Lond A 2003;361(1806): 965–86.
[55] Kachanov LM. Foundations of the theory of plasticity. Amsterdam: North-Holland; 1971.
[56] Huet C. An integrated micromechanics and statistical continuum thermodynamics approach for studying the fracture behaviour of microcracked heterogeneous materials with delayed response. Eng Fract Mech 1997;58(5–6):459.
[57] Huet C. Coupled size and boundary conditions effects in viscoelastic heterogeneous and composite bodies. Mech Mater 1999;31:787–829.
[58] Rosen BW, Hashin Z. Effective thermal expansion coefficients and specific heats of composite materials. Int J Eng Sci 1970;8:157–73.
[59] Christensen RM. Mechanics of composite materials.: Krieger Publ. Co; 1991.
[60] Du X. PhD Thesis (in progress). Canada: McGill University;2005.
[61] Du X, Ostoja-Starzewski M. Mesoscale bounds on effective thermal expansion of random composites 6th International congress of thermal stresses and related topics. Austria: Vienna; 2005 pp. 755–758.
[62] Dullien FAL. Porous media: fluid transport and pore structure.: Academic Press; 1979.
[63] Berryman JG, Milton GW. Normalization constraint for variational bounds on fluid permeability. J Chem Phys 1985;83(2):754–60.
[64] Chung TJ. Computational fluid dynamics.: Cambridge University Press; 2000.
[65] Ziegler H. An introduction to thermomechanics. Amsterdam: North-Holland; 1983.
[66] Maugin GA. The thermomechanics of nonlinear irreversible behaviors—an introduction. Singapore: World Scientific; 1999.
[67] Ostoja-Starzewski M. Microstructural randomness versus representative volume element in thermomechanics. ASME J Appl Mech 2002;69: 25–35.
[68] Ostoja-Starzewski M. Towards stochastic continuum thermodynamics. J Non-Equilib Thermodyn 2002;27(4):335–48.
[69] Willis JR. Variational and related methods for the overall properties of composites. Adv Appl Mech 1981;21:1–78.
[70] Hill R. On constitutive macro-variables for heterogeneous solids at finite strain. Proc R Soc Lond A 1972;326:131–47.
[71] Ponte Castañeda P, Suquet PM. Nonlinear composites. Adv Appl Mech 1998;34:171–302.
[72] Ren ZY, Zheng QS. A quantitative study on minimum sizes of representative volume elements of cubic polycrystals - numerical experiments. J Mech Phys Solids 2002;50:881–93.
[73] Ren ZY, Zheng QS. Effects of grain sizes, shapes and distribution on minimum sizes of representative volume elements of cubic polycrystals—numerical experiments. Mech Mater 2004;36:1217–29.
[74] Kouznetsova V, Geers MGD, Brekelmans WAM. Multi-scale constitutive modelling of heterogeneous materials with a gradient-enhanced computational homogenization scheme. Int J Numer Meth Engng 2002;54: 1235–60.
[75] Kouznetsova V, Geers MGD. Brekelmans WAM, Size of a representative volume element in a second-order computational homogenization framework. Int J Multiscale Comput Eng 2004;2(4):575–98.
[76] Kouznetsova V, Geers MGD. Brekelmans WAM, Multi-scale second-order computational homogenization of multi-phase materials: a nested finite element solution strategy. Comp Meth Appl Mech Eng 2004;193: 5525–50.